Multiprotein assembly of Kv4.2, KChIP3 and DPP10 produces ternary channel complexes with I_{SA}-like properties

Henry H. Jerng[1], Kumud Kunjilwar[2] and Paul J. Pfaffinger[1]

[1] *Department of Neuroscience, Baylor College of Medicine, Houston, TX 77030, USA*
[2] *Department of Integrative Biology and Pharmacology, University of Texas – Houston Medical School, Houston, TX 77030, USA*

Kv4 pore-forming subunits are the principal constituents of the voltage-gated K^+ channel underlying somatodendritic subthreshold A-type currents (I_{SA}) in neurones. Two structurally distinct types of Kv4 channel modulators, Kv channel-interacting proteins (KChIPs) and dipeptidyl-peptidase-like proteins (DPLs: DPP6 or DPPX, DPP10 or DPPY), enhance surface expression and modify functional properties. Since KChIP and DPL distributions overlap in the brain, we investigated the potential coassembly of Kv4.2, KChIP3 and DPL proteins, and the contribution of DPLs to ternary complex properties. Immunoprecipitation results show that KChIP3 and DPP10 associate simultaneously with Kv4.2 proteins in rat brain as well as heterologously expressing *Xenopus* oocytes, indicating Kv4.2 + KChIP3 + DPP10 multiprotein complexes. Consistent with ternary complex formation, coexpression of Kv4.2, KChIP3 and DPP10 in oocytes and CHO cells results in current waveforms distinct from the arithmetic sum of Kv4.2 + KChIP3 and Kv4.2 + DPP10 currents. Furthermore, the Kv4.2 + KChIP3 + DPP10 channels recover from inactivation very rapidly (τ_{rec} ~18–26 ms), closely matching that of native I_{SA} and significantly faster than the recovery of Kv4.2 + KChIP3 or Kv4.2 + DPP10 channels. For comparison, identical triple coexpression experiments were performed using DPP6 variants. While most results are similar, the Kv4.2 + KChIP3 + DPP6 channels exhibit inactivation that slows with increasing membrane potential, resulting in inactivation slower than that of Kv4.2 + KChIP3 + DPP10 channels at positive voltages. In conclusion, the native neuronal subthreshold A-type channel is probably a macromolecular complex formed from Kv4 and a combination of both KChIP and DPL proteins, with the precise composition of channel α and auxiliary subunits underlying tissue and regional variability in I_{SA} properties.

(Received 31 March 2005; accepted after revision 22 August 2005; first published online 25 August 2005)
Corresponding author H. H. Jerng: Department of Neuroscience, Baylor College of Medicine, One Baylor Plaza, S630, Houston, TX 77030, USA. Email: hjerng@cns.bcm.tmc.edu

The somata and dendrites of neurones possess subthreshold A-type K^+ currents (I_{SA}) with distinct time- and voltage-dependent properties essential for neurophysiology (reviewed by Jerng *et al.* 2004*b*). Rapid activation, inactivation and recovery from inactivation at subthreshold membrane potentials collectively allow I_{SA} to influence neuronal excitability, spike repolarization and frequency of repetitive firing (Connor & Stevens, 1971; Baxter & Byrne, 1991; Hille, 2001). In dendrites, I_{SA} actively serves to coordinate the integration of synaptic signals, control back propagation of action potentials, and regulate the induction of long-term potentiation (Hoffman *et al.* 1997; Schoppa & Westbrook, 1999; Johnston *et al.* 2000; Watanabe *et al.* 2002).

The overwhelming majority of somatodendritic I_{SA} is evidently expressed by K^+ channels assembled from the homo- or heteromultimerization of Kv4 pore-forming α-subunits (Johns *et al.* 1997; Shibata *et al.* 2000; Malin & Nerbonne, 2000). To produce mature subthreshold A-type channels, the Kv4 subunits probably form complexes with modulatory accessory proteins. Immunoprecipitation of Kv4.2 complexes from brain membrane extracts has highlighted two important families of Kv4-associated proteins: Kv-channel-interacting proteins (KChIPs) and dipeptidyl-aminopeptidase-like proteins (DPPX, DPP10) (Nadal *et al.* 2003; Zagha *et al.* 2005). KChIPs (KChIP1-4) are Ca^{2+}-binding proteins related to the neuronal Ca^{2+}

H. H. Jerng and K. Kunjilwar contributed equally to this work.

DOI: 10.1113/jphysiol.2005.087858

sensor (NCS), and they bind the cytoplasmic N-terminus of Kv4 channels, typically increasing surface trafficking and remodelling gating behaviour (An *et al.* 2000; Bähring *et al.* 2001*a*; Beck *et al.* 2002; Holmqvist *et al.* 2002; Zhou *et al.* 2004). Interestingly, as a putative multifunctional protein, KChIP3 has also been identified as a presenilin-binding protein (calsenilin) and a transcription factor regulating dynorphin expression (downstream regulatory element antagonist modulator, DREAM) (Buxbaum *et al.* 1998; Carrion *et al.* 1999). As such, knockout of KChIP3 in mouse has been shown to downregulate I_{SA}, enhance long-term potentiation, reduce amyloid β-peptide levels, and dampen response to pain (Lilliehook *et al.* 2003; Cheng *et al.* 2002). In brain, KChIP3 mRNA and protein are particularly abundant in the dentate gyrus of hippocampus, piriform cortex and cerebellar granule cells (Spreafico *et al.* 2001; Lilliehook *et al.* 2003).

DPP6 (also known as BSPL, DPPX and DPL1) and the related DPP10 (also known as KIAA1492, DPRP3, DPL2 and DPPY) both associate with Kv4 channels, facilitating surface expression and modifying channel kinetic and steady-state properties (Wada *et al.* 1992; de Lecea *et al.* 1994; Nagase *et al.* 2000; Chen *et al.* 2003; Nadal *et al.* 2003; Qi *et al.* 2003; Jerng *et al.* 2004*a*; Strop *et al.* 2004; Zagha *et al.* 2005). In this study, we used the MEROPS database designations of DPP6 and DPP10 (Barrett *et al.* 2001) and we refer to them both as DPLs ('dipeptidyl-peptidase-like' proteins). DPP6 and DPP10 are integral membrane glycoproteins with a short cytoplasmic N-terminal domain, one transmembrane domain, and a long extracellular C-terminal domain (Wada *et al.* 1992; Kin *et al.* 2001; Qi *et al.* 2003). Alternative splicing of the N-terminal domain of DPP6 produces three isoforms: two adult forms (DPP6-S and DPP6-L) and one embryonic form (Wada *et al.* 1992; Hough *et al.* 1998). Although they are members of the dipeptidyl aminopeptidase family, neither DPP6 nor DPP10 possesses peptidase activity (Kin *et al.* 2001; Qi *et al.* 2003). Enzymatic inactivity may be attributed to replacement of the catalytic serine by aspartate and glycine in DPP6 and DPP10, respectively, but introduction of the serine in DPP6-S by mutagenesis fails to restore activity. Both DPP6 and DPP10 are widely expressed in brain. In rat, DPP6 transcripts are enriched in hippocampus, striatum and thalamus, while DPP10 transcripts are prominent in the cortex, olfactory bulb, thalamus and specific populations in the cerebellum (Wada *et al.* 1992; de Lecea *et al.* 1994; Zagha *et al.* 2005). In human, DPP10 transcripts show conspicuous expression in most brain regions except cerebellum (Nagase *et al.* 2000; Allen *et al.* 2003).

In areas where Kv4, KChIP and DPL expression patterns prominently overlap, ternary channel complexes may conceivably assemble and contribute significantly to the total Kv4-mediated I_{SA}. Some Kv4 channel complexes from rat cerebellum probably contain both KChIP and DPP6 proteins because antibodies against KChIPs immunoprecipitate DPP6, and antibodies against DPP6 immunoprecipitate KChIPs (Nadal *et al.* 2003). Coexpression of Kv4.2 with both DPP6-S and KChIP1 in *Xenopus* oocytes produces currents with a mixture of properties of Kv4.2 + KChIP1 and Kv4.2 + DPP6-S currents (Nadal *et al.* 2003). To further investigate the possibility of Kv4 + KChIP + DPL ternary complexes, we have tested protein–protein interactions by immunoprecipitation, and studied K^+ currents from *Xenopus* oocytes and Chinese hamster ovary (CHO) cells expressing Kv4.2, KChIP3 and DPLs (DPP6-S, DPP6-L and DPP10). To the best of our knowledge, we are the first to report here that Kv4.2, DPP10 and KChIP3 proteins from rat brain, as well as those heterologously expressed in oocytes, assemble into ternary complexes. In CHO cells, DPP10 enhances Kv4.2 current expression and altered kinetic and steady-state properties in ways similar to those observed previously in *Xenopus* oocytes (Jerng *et al.* 2004*a*). The coexpression of Kv4.2, KChIP3, and either DPP6 or DPP10 in oocytes and CHO cells, yields novel properties, consistent with K4.2 + KChIP3 + DPL ternary complex formation. Most notable is the added acceleration of recovery from inactivation (τ_{rec} ~18–26 ms at −100 mV) with coexpression of both KChIP3 and DPLs. Dramatically different inactivation kinetics is observed in CHO cells and oocytes between Kv4.2 + KChIP3 + DPP6 and Kv4.2 + KChIP3 + DPP10 channels, suggesting that in the presence of KChIPs the identity of the associated DPL plays a crucial role in gating modulation. In conclusion, the assembly of Kv4 with distinct KChIPs and DPLs critically contributes to the generation of I_{SA} in neurones, and may provide an additional basis for I_{SA} waveform variability in different regions of the brain.

Methods

Molecular biology

Rat Kv4.2 cDNA in the pBluescript SK vector (pBS-SK/rKv4.2) was a generous gift from Dr Lily Jan (University of California at San Francisco, CA, USA). Human KChIP3 in pT7T3D-Pac (pT7T3D-Pac/hKChIP3) and DPP10 in pBSR (pBSR/hDPP10) were purchased from the American Type Culture Collection (ATCC, Manassas, VA, USA). The generation of human DPP6-S (pT7T3D-Pac/DPP6-S), human DPP6-L (pT7T3D-Pac/DPP6-L), and N-terminal HA-tagged hDPP10 (pBSR/HA/hDPP10) have been previously described (Jerng *et al.* 2004*a*). N-terminal HA-tagging of hKChIP3 was performed by PCR using a forward primer nested with the HA-coding sequence (5′-TAC, CCA, TAC, GAT, GTT, CCA, GAT, TAC, GCT-3′). Kv4.2, KChIP3, DPP10, DPP6-S and DPP6-L coding regions were subcloned using recombinant DNA techniques

into pCMV-based vectors for expression in CHO cells. All DNA constructs were confirmed and verified by automated sequencing (DNA sequencing core facility of Baylor College of Medicine, Houston, TX, USA). For expression in oocytes, run-off cRNA transcripts were synthesized from linearized DNAs using the mMESSAGE mMACHINE high-yield capped RNA transcription kit (Ambion, Austin, TX, USA).

Immunoprecipitation and Western blotting

Solubilized membrane extracts from rat cortex, cerebellum, and hippocampus were prepared as previously described (Nadal *et al.* 2003). Sprague-Dawley rats were anaesthetized by isofluorane inhalation and rapidly killed by cervical dislocation, in accordance with the Animal Welfare Act, Public Health Services Animal Welfare Policy, National Institutes of Health Guide for Care and Use of Laboratory Animals, and Baylor College of Medicine regulations. Our method for immunoprecipitation of heterologously expressed proteins from *Xenopus* oocytes, aside from modifications for protein cross-linking, has been described in detail elsewhere (Jerng *et al.* 2004*a*). Cross-linking of Kv4.2 with DPP6 and KChIP by dimethyl 3,3′-dithiobispropionimidate (DTBP; Pierce, Rockford, IL, USA) prior to membrane solubilization better preserved protein–protein interactions (Nadal *et al.* 2003). DTBP, a membrane-permeable homobifunctional reagent with disulphide linkages, reacts with free amino groups. To cross-link proteins, prior to disruption, oocytes were washed twice with HEPES buffer (50 mM HEPES, pH 7.5, 150 mM KCl) and then incubated in HEPES solution containing freshly prepared 0.5 mg ml^{-1} DTBP for 1 h at room temperature. The disulphide linkage in DTBP is cleaved by reduction with dithiothreitol (DTT, 0.1 M) present in the SDS-PAGE loading buffer. In accordance with previous findings, we too observed that association of Kv4.2 with KChIP3 and DPP10 was retained better (by approximately 2–3 times) if they were chemically cross-linked.

Immunoprecipitated proteins were separated using SDS-PAGE, transferred to polyvinylidene fluoride (PVDF) membranes (Immobilon; Millipore, Bedford, MA, USA), and probed with specific primary antibodies as indicated. Immunoblots were incubated with the appropriate primary antibody for at least 2 h, and with the secondary HRP-conjugated antibodies for 1 h at room temperature. The bound antibodies were detected by chemiluminescence with an ECL detection kit (Pierce). Anti-Kv4.2 (AB5360; Chemicon International, Temecula, CA, USA), anti-KChIP3 (FL-214; Santa Cruz Biotechnology, Santa Cruz, CA, USA), anti-DPP10 (COO-12; a gift of Dr William O. Cookson), and anti-HA antibodies (3F10; Roche Diagnostics Corporation, Indianapolis, IN, USA) were used at 1:1000, 1:1000, 1:500 and 1:100 dilutions, respectively. In DTBP cross-linked samples, a secondary higher-molecular-mass band (~220 kDa) was detected by the DPP10 antibody in addition to the main ~97 kDa form. The ~220 kDa band probably represents residual DPP10 dimers with uncleaved DTBP cross-links.

Heterologous expression in *Xenopus* oocytes and CHO cells

Defolliculated oocytes at stages V and VI of development were injected with Kv4.2 cRNA alone (2–4 ng $oocyte^{-1}$) or mixed with equimolar amounts of KChIP3 cRNA, DPL cRNA, or both. Following a protocol approved by the Institutional Animal Care and Use Committees (IACUC), *Xenopus laevis* frogs were anaesthetized with 0.1% tricaine solution absorbed through the skin, and oocytes were harvested through a small incision that was sutured following surgery. The frogs were then placed back in the vivarium for daily monitoring, and allowed to recover for at least 2 weeks before a second surgery was performed. Spent frogs were killed by double pithing under anaesthesia. Injections were performed using a Nanoinjector (Drummond, Broomall, PA, USA), and injected oocytes were maintained at 18°C in standard ND96 solution (mM: 96 NaCl, 2 KCl, 1.8 $CaCl_2$, 1 $MgCl_2$ and 5 HEPES, pH 7.4) supplemented with 5 mM sodium pyruvate and 5 μg ml^{-1} gentamicin. Whole oocyte currents were measured 1–3 days post injection.

CHO-K1 cells were cultured in DMEM medium supplemented with 10% FBS, 40 μg ml^{-1} L-proline, 100 U ml^{-1} penicillin and 100 U ml^{-1} streptomycin. Following the manufacturer's protocol, lipofectamine (Gibco-BRL) was used to transiently transfect CHO cells with appropriate cDNAs. As previously described, cells were plated on glass coverslips and transfected at optimal confluency (~50–60%) (Kunjilwar *et al.* 2004). The lipofectamine transfection approach limited total cDNA per reaction to 4.5 μg, with 0.5 μg reserved for enhanced green fluorescent (EGFP; Clonetech) as a means to assess transfection efficiency and identify cells for recording. Amounts of KChIP3, DPP10, DPP6-S and DPP6-L cDNAs were equal to that of Kv4.2 (either at 0.8 or 0.4 μg), and the total cDNA level was adjusted with red fluorescent protein (RFP) cDNA. Recordings from CHO cells were done 18–20 h after transfection.

Solutions and electrophysiological recordings

Whole-oocyte currents were recorded at room temperature (~22–23°C) using two-electrode voltage clamp as previously described (Oocyte Clamp; Warner Instruments, Hamden, CT, USA; Jerng *et al.* 2004*a*). Pulled microelectrodes with tip resistance of <1 MΩ

were back-filled with 3 M KCl and used to impale oocytes bathed in normal ND96 solution. The voltage-clamp protocols were managed by pClamp6 (Axon Instruments, Union City, CA, USA), and the data were appropriately digitized and lowpass filtered before their acquisition. The electrode offsets were typically <2 mV after recordings. The capacitative transients and leak currents (<0.2 μA) were either subtracted on-line using a P/4 protocol (200 ms pulses) or off-line by assuming Ohmic leak and subtracting scaled up transients at voltages without ionic currents (at −90 mV).

Whole-cell currents from transfected CHO cells were measured with an Axopatch-200B amplifier (Axon Instruments) in the whole-cell patch configuration (refer to Kunjilwar *et al.* 2004). Cells expressing EGFP were identified by fluorescence microscopy and selected for recordings. Micropipettes with resistance of 0.9–1.2 MΩ were filled with (mM) 140 KCl, 0.133 $CaCl_2$, 1 $MgCl_2$, 1 EGTA, 10 HEPES (pH 7.4). The bath solution contained the following (mM): 2 KCl, 138 NaCl, 1.8 $CaCl_2$, 1 $MgCl_2$, 10 HEPES (pH 7.4). Under these conditions, the reversal potential was ∼−90 mV, the same as that of oocyte recording using ND96. Currents were sampled at 5 kHz and filtered at 2 kHz, and series resistance was compensated by 90–95%. Leak subtraction was performed on-line by using a P/8 protocol. CHO cells recordings were conducted at room temperature (25 ± 2°C).

Data acquisition and analysis

Digitized data from two-electrode voltage-clamp and patch-clamp recordings were acquired and stored on desktop PC using pClamp6 and pClamp7, respectively (Axon Instruments). Current traces were analysed with Clampfit (Axon Instruments) and Origin software (OriginLab Corp., Northampton, MA, USA). Time course of current decays was described as either time at half-inactivation ($t_{0.5}$) or the sum of multiexponential terms using Clampfit or Origin. Published time constants were converted to half-inactivation time using the following equation:

$$t_{0.5} = \ln 0.5/-\tau$$

where τ is the time constant. In exponential fitting, the left cursor was placed at the time point with the fastest change in the declining phase of the current, as determined by differentiating the current trace. The right cursor was placed at the end of the traces. Peak conductance (G_p) was calculated as:

$$G_p = I_p/(V_c - V_{rev})$$

where I_p is the peak current, V_c is the command voltage, and V_{rev} is the reversal potential (−90 to −95 mV in ND96). Peak conductance–voltage (G_p–V) curves were fitted for comparison using the first-order Boltzmann function:

$$G_p/G_{pmax} = 1/\{1 + \exp[(V_m - V_a)/k]\}$$

where G_p/G_{pmax} is the fraction of maximal conductance, V_m is the given membrane potential, V_a is the potential for half-maximal activation, and k is the slope factor. Steady-state inactivation curves were also described by a simple first-order Boltzmann function. Pooled data are presented as means ± S.E.M., and the two-tailed Student's t test for unpaired data was applied to determine if a variable significantly differed between control and experimental groups. Differences were considered statistically significant when $P < 0.05$.

Results

Kv4.2 proteins are associated with KChIP3 and DPP10 proteins in rat cortex, cerebellum and hippocampus, and some Kv4.2 complexes contain both KChIP3 and DPP10 proteins

The distribution pattern of DPP10 message in brain has previously been analysed by *in silico* expressed sequence tag (EST) screens, Northern hybridization, RT-PCR ELISA and *in situ* hybridization (Nagase *et al.* 2000; Qi *et al.* 2003; Allen *et al.* 2003; Zagha *et al.* 2005). Those studies suggest that DPP10, KChIP3 and Kv4 gene expressions overlap in various regions of the brain, including the cortex, cerebellum and hippocampus (Table 1). To determine whether DPP10 proteins are expressed in these regions and whether they associate with Kv4 and KChIP3 in neuronal membranes, we prepared nondenaturing detergent extracts of rat cortical, cerebellar and hippocampal membranes and immunoprecipitated them with goat anti-Kv4.2 antibodies and protein A/G beads, followed by elution, separation by SDS-PAGE, and transfer to Immobilon membranes.

Western blotting of the total extracts from rat cortex, cerebellum and hippocampus showed that DPP10 proteins were expressed in these regions (Fig. 1*Aa*). We used the COO-12 anti-DPP10 polyclonal antibodies, which have previously been used to successfully detect DPP10 coprecipitated with Kv4.2 from rat brain extracts (Zagha *et al.* 2005). The antibodies specifically bind DPP10 proteins heterologously expressed in oocytes (discussed later), and they do not cross-react with the closely related DPP6 proteins (H. H. Jerng, unpublished observations). The anti-DPP10 antibodies detected an intense band of ∼97 kDa that corresponds with DPP10 heterologously expressed in oocytes (Jerng *et al.* 2004*a*; Fig. 2*A*). Probing the immunoblots with anti-KChIP3 and anti-Kv4.2 antibodies revealed that KChIP3 and Kv4.2 proteins were

Table 1. Expression patterns of Kv4.2, KChIPs, DPP6 and DPP10 in rodents

Brain region	Kv4.2/Kv4.3	KChIP3	DPP6	DPP10	KChIP1	KChIP2	KChIP4
Neocortex							
Layer I		−			++		
Layer II–III	+++	++	+++	++++	+	++	++++
Layer IV	++	+	++	++	+	++++	+++
Layer V	+++	+	+++	++++	+	++	+++
Layer VIa	++	++++	++	+++	+	+	++
Layer VIb	++	++++	++	+++	−	+++	+++
Hippocampus							
CA1	++++/+	+	++++	+	+	+++	++++
CA2	++/++		++++	+	+	+++	
CA3	++/++	+	++++	+	+	+++	++
Dentate gyrus	++++/++++	++++	++++	+	+	++++	+
Thalamus	+++/+++	+++	+++	+++	+++	+/−	+++
Cerebellum							
Granule cells	++++/+++	++++	+++	++	++	−	−
Purkinje cells	−/++++	+++	++	++++	++++	−	++++

−, Not detectable; +, low level of expression; ++, low to moderate level of expression; +++, moderate to high level of expression; +++, high to very high level of expression. Kv4.2/Kv4.3: Serodio & Rudy (1998); Rhodes *et al.* (2004). KChIP1: An *et al.* (2000); Rhodes *et al.* (2004); Xiong *et al.* (2004). KChIP2: An *et al.* (2000); Rhodes *et al.* (2004); Xiong *et al.* (2004). KChIP3: Spreafico *et al.* (2001); Lilliehook *et al.* (2003); Rhodes *et al.* (2004); Xiong *et al.* (2004). KChIP4: Holmqvist *et al.* (2002); Rhodes *et al.* (2004); Xiong *et al.* (2004). DPP6: de Lecea *et al.* (1994); Wada *et al.* (1992); Zagha *et al.* (2005). DPP10: Zagha *et al.* (2005).

also expressed in all three brain regions (Fig. 1*Ab* and *Ac*). Staining for KChIP3 resulted in the appearance of two bands, which may represent alternative splice variants or products of post-translational modifications or proteolytic degradations (Zaidi *et al.* 2002). Western blots probed with anti-Kv4.2 antibody showed three bands corresponding to the monomer (∼65 kDa) and known aggregates as previously described (Fig. 1*Ac*; Jerng *et al.* 2004*a*). Figure 1*Aa* and *Ab* also shows the results of staining proteins immunoprecipitated with goat anti-Kv4.2 antibodies for DPP10 and KChIP3. Kv4.2; KChIP3 and DPP10 proteins were coimmunoprecipitated by anti-Kv4.2 antibodies, but not by control goat IgG antibodies (Fig. 1*Aa* and *Ac*).

Thus, Kv4.2 proteins associate with DPP10 and KChIP3 in neuronal membranes from cortex, cerebellum and hippocampus. To determine if Kv4.2 can form a complex with both DPP10 and KChIP3, we performed immunoprecipitation of cortical membrane extracts using rabbit anti-KChIP3 antibodies and probed the immunoblot with rabbit anti-DPP10 antibodies (Fig. 1*B*). The immunoblot showed that DPP10 proteins were immunoprecipitated by anti-KChIP3 antibody (Fig. 1*B*, indicated by an arrow), suggesting that some Kv4.2 protein complexes contain both KChIP3 and DPP10. The reciprocal coimmunoprecipitation could not be conducted since the anti-DPP10 antibody (COO-12) was useful only for immunoblots (Zagha *et al.* 2005).

Immunoprecipitation of a supermolecular complex containing Kv4.2, KChIP3 and DPP10 proteins expressed in *Xenopus* oocytes

Our coimmunoprecipitation results from brain support a reasonable hypothesis that Kv4 proteins associate with DPP10 without losing their ability to bind KChIPs, thereby resulting in a supermolecular complex containing two distinct auxiliary subunits. Previously, Nadal and colleagues similarly proposed that Kv4.2 channel complexes from rat cerebellum might possess both DPP6 and KChIPs, since anti-DPP6 antibodies immunoprecipitate KChIPs and vice versa (Nadal *et al.* 2003). However, the biochemical argument for Kv4.2, DPP6 and KChIP forming triple complexes remains inconclusive, without evidence to show that DPP6 and KChIPs do not directly interact among themselves. To directly test this possibility, we used *Xenopus* oocytes to heterologously express DPP10 and KChIP3 in the presence and absence of Kv4.2, and subsequently performed immunoprecipitation and Western analysis to determine the conditions for integration of DPP10 and KChIP3 into the same protein complex. Since N-terminal HA-tagged DPP10 (HA/DPP10) has been demonstrated to effectively bind and coimmunoprecipitate with Kv4.2 proteins (Jerng *et al.* 2004*a*), we generated a construct expressing KChIP3 with HA genetically fused at its N terminus (HA/KChIP3) and then used anti-HA antibody to precipitate HA/DPP10 or HA/KChIP3.

Antibody specificities were checked by reacting anti-Kv4.2, anti-KChIP3 and anti-DPP10 antibodies against blots containing non-denaturing detergent extracts from uninjected oocytes and oocytes expressing the proteins in question. As Fig. 2*A* shows, these antibodies detected their respective target proteins. Western blots probed with anti-Kv4.2 antibody showed the Kv4.2 band pattern seen in Fig. 1*Ac*, as explained previously. Anti-KChIP3 antibody detects monomeric KChIP3 as a single band at ∼32 kDa that corresponds to the main KChIP3 band in rat brain. Anti-DPP10 antibody showed monomeric DPP10 at ∼97 kDa, consistent with previous findings (Jerng *et al.* 2004*a*). Through N-terminal tagging of DPP10 with the HA epitope, the detection of the same protein band by anti-HA and anti-DPP10 antibodies further asserted the specificity of anti-DPP10 antibodies (Fig. 2*B*). Subsequently, extracts were prepared from oocytes expressing pairs of auxiliary subunits (either HA/KChIP3 and DPP10, or KChIP3 and HA/DPP10), in the presence and absence of Kv4.2. Prior to detergent solubilization, oocytes were treated with freshly prepared DTBP to chemically cross-link membrane complexes to better preserve their interactions, as suggested previously (Nadal *et al.* 2003). Goat IgG (control), and anti-HA and anti-Kv4.2 antibodies were added in parallel to aliquots of the extracts to immunoprecipitate Kv4.2 complexes.

Figure 2*C* and *D* shows the results of Western detection by anti-DPP10, anti-KChIP3, anti-Kv4.2 and anti-HA

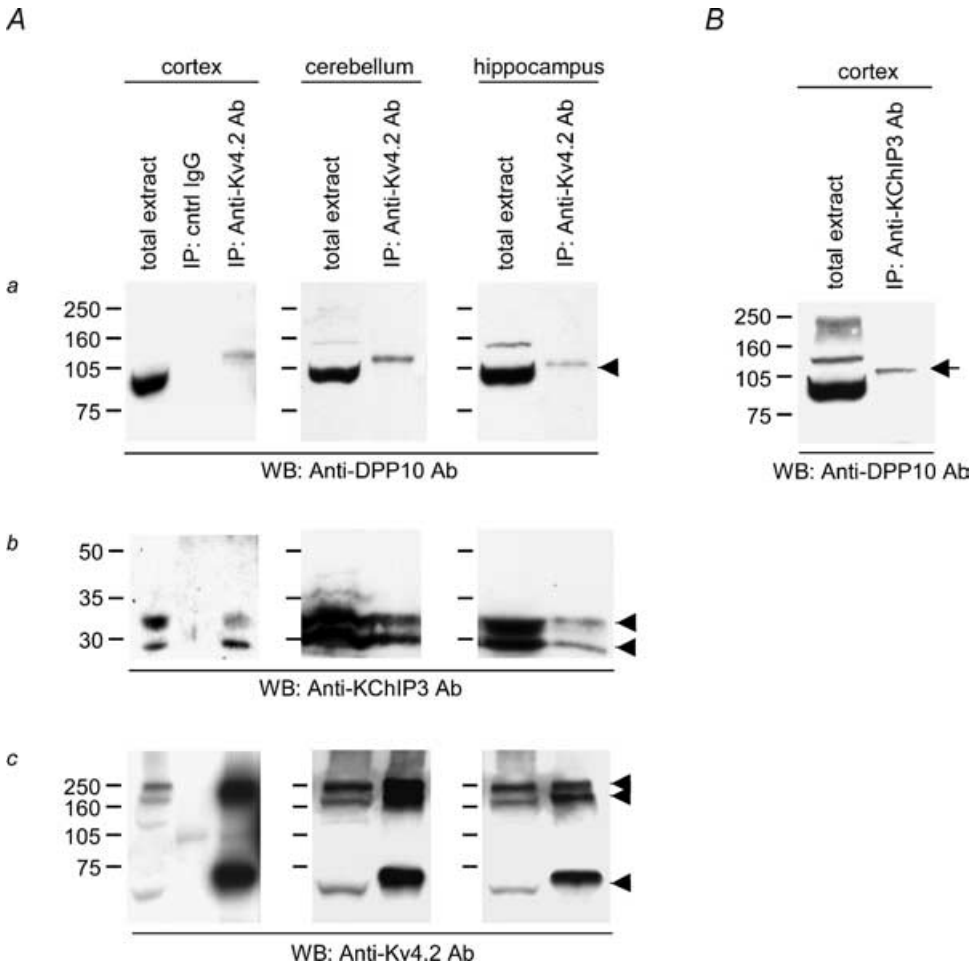

Figure 1. Kv4.2 proteins are associated with DPP10 and KChIP3 proteins in rat cortex, cerebellum and hippocampus, and some Kv4.2 complexes contain both DPP10 and KChIP3 proteins
A, coimmunoprecipitation of Kv4.2, KChIP3 and DPP10. Non-denaturing detergent extracts of membrane preparations from various regions of rat brain were subjected to immunoprecipitation using anti-Kv4.2 antibody and/or control (cntrl) IgG. Immunoprecipitated proteins were dissociated, separated on SDS-PAGE, and transferred onto an Immobilon membrane. The blots were probed with anti-DPP10 antibody (*a*), anti-KChIP3 antibody (*b*) and anti-Kv4.2 antibody (*c*). *B*, anti-KChIP3 antibodies immunoprecipitate DPP10. Immunoprecipitation products were probed with anti-KChIP3 antibody. Arrowheads point to the expected molecular masses of respective proteins, and the arrow indicates the DPP10 band coimmunoprecipitated by anti-KChIP3 antibody. IP, immunoprecipitation; WB, Western blot.

antibodies. Detection by anti-HA antibodies was used to confirm the results obtained by the COO-12 anti-DPP10 antibodies in the triple coexpression context. As expected, the anti-Kv4.2 antibody immunoprecipitated both DPP10 and KChIP3, irrespective of whether or not they had N-terminal HA tags (in the anti-Kv4.2 lane: Fig. 2*Ca* for DPP10, Fig. 2*Da* for HA/DPP10, Fig. 2*Db* for KChIP3, and Fig. 2*Cb* for HA/KChIP3). After immunoprecipitation, both DPP10 and HA/DPP10 proteins reproducibly exhibited an apparent increase in molecular mass as compared with the starting extract material (Fig. 2*Ca*, *Da* and *Dd*). The difference in size is likely to result from a differential amount of total protein loaded per lane. The total protein loaded after immunoprecipitation was markedly less than that for the extract material (~1.3 mg per lane), resulting in prominent 'smiling' of the extract DPP10 bands. Judging by the intensity of the coprecipitated DPP10 as well as the KChIP3 bands, the presence of the HA tag has no significant effect on the association between the auxiliary subunits and the Kv4.2 α-subunits.

Finally, anti-HA antibody specifically immunoprecipitated HA-tagged proteins, as shown by precipitation experiments with HA/KChIP3 + DPP10 and HA/DPP10 + KChIP3. From extract containing HA/KChIP3 and DPP10 without Kv4.2, anti-HA antibody pulled down HA/KChIP3 but not DPP10 (Fig. 2*Cb* and *Ca*), and from extract containing HA/DPP10 and KChIP3 without Kv4.2, anti-HA antibody pulled down HA/DPP10 but not KChIP3 (Fig. 2*Db* and *Da*). These results conclusively show that DPP10 and KChIP3 do not associate with each other. However, when Kv4.2 is coexpressed with DPP10 and KChIP3 (either Kv4.2 + HA/KChIP3 + DPP10, or Kv4.2 + KChIP3 + HA/DPP10), anti-HA antibody immunoprecipitated all three proteins, indicating that they assemble into a triple complex (Fig. 2*Ca*, *Cc*, *Da*, *Db* and *Dc*). In short, given that Kv4 protein is present, antibodies against one auxiliary subunit can precipitate out the other auxiliary subunit (indicated by arrows in Fig. 2*Ca* and *Db*). The same set of experiments conducted without chemical cross-linking shows identical results, but with less protein coprecipitated (H. H. Jerng, unpublished observations).

Currents mediated by the coexpression of Kv4.2, KChIP3 and DPP10 exhibit distinct inactivation and recovery kinetics, consistent with the formation of ternary complex in *Xenopus* oocytes

We next investigated the effects of dual auxiliary subunits on Kv4 channel function by examining Kv4 currents generated by heterologous coexpressions in *Xenopus* oocytes (Fig. 3). Equal molar amounts of α- and auxiliary subunit cRNAs were coinjected into individual oocytes with expectations of similar levels of expressed proteins. The coexpression of KChIP3 and DPP10 increased the Kv4.2-mediated current on average by ~6.4- and 5.8-fold, respectively. The increased current expression associated with KChIP and DPP10 is due to facilitation of Kv4.2 protein trafficking to the cell surface (Bähring *et al.* 2001*a*; Jerng *et al.* 2004*a*; Zagha *et al.* 2005). Oocytes coinjected with Kv4.2, KChIP3 and DPP10 cRNAs had A-type currents with amplitudes approximately four times greater than those injected with Kv4.2 alone. This increase is not statistically different from those observed with KChIP3 and DPP10 coexpression, suggesting no recruitment of additional channels to the surface by the triple complex.

KChIP3 and DPP10 dramatically alter Kv4.2 current waveforms: KChIP3 markedly slowed the inactivation time course, whereas DPP10 accelerated it (Fig. 3*A*). Inspection of the Kv4.2 + KChIP3 + DPP10 traces revealed relatively modest differences from those of Kv4.2 + DPP10 channels (Fig. 3*A*). As the normalized overlapped traces show, the addition of KChIP3 to the Kv4.2 + DPP10 binary complex resulted primarily in a slight slowing of inactivation, with the Kv4.2 + KChIP3 + DPP10 current inactivating significantly faster than that of Kv4.2 alone (Fig. 3*B*, left panel). We measured the time at which half of the current inactivates ($t_{0.5}$) at +50 mV, and the values were 33.1 ± 1.8 (Kv4.2), 109 ± 2.3 (Kv4.2 + KChIP3), 8.0 ± 0.7 (Kv4.2 + DPP10) and 11.8 ± 1.8 ms (Kv4.2 + KChIP3 + DPP10) ($n = 15$, 6, 7 and 7, respectively). This indicates that DPP10 has a dominating effect over channel inactivation, which is a critical feature if DPP10 is to restore native subthreshold A-type-like inactivation to KChIP-bound Kv4.2 channels with slowed inactivation. The kinetics of the observed Kv4.2 + KChIP3 + DPP10 current was consistent with that of a triple complex, since they were distinct from an arithmetic sum of the Kv4.2 + DPP10 and Kv4.2 + KChIP3 currents at 1:1, 2:1 or 1:2 ratios (Fig. 3*B*, right panel).

As a further indication of ternary complex formation, the concerted actions of KChIP3 and DPP10 accelerated the kinetics of Kv4.2 recovery from inactivation significantly more than either subunit alone (Fig. 3*C*). The time courses of recovery from inactivation at −100 mV, as determined by monoexponential fittings, had time constants of 238 ± 31 (Kv4.2), 77 ± 3 (Kv4.2 + KChIP3), 79 ± 13 (Kv4.2 + DPP10), and 24 ± 7 ms (Kv4.2 + KChIP3 + DPP10) ($n = 21$, 9, 9 and 5, respectively). This indicates that individual coexpression of KChIP3 or DPP10 in oocytes accelerates Kv4.2 recovery from inactivation by approximately threefold, whereas a combination of KChIP3 and DPP10 produces ~10-fold acceleration. These results indicate that the addition of KChIP3 to Kv4.2 + DPP10 channels affects inactivation kinetics modestly, but markedly boosts recovery from

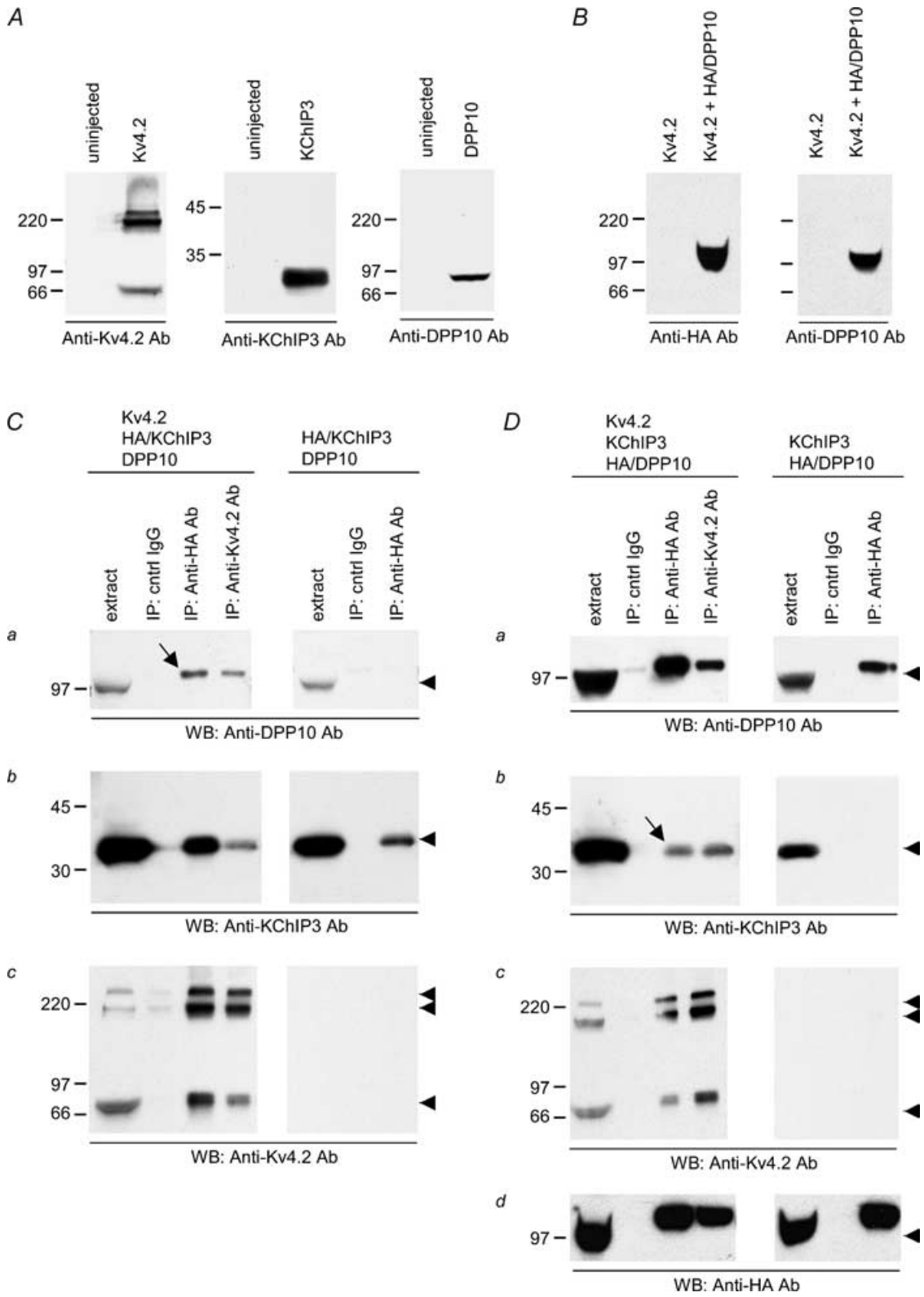

Figure 2. Formation of a protein complex containing both DPP10 and KChIP3 requires Kv4.2 coexpression
A, anti-Kv4.2, anti-KChIP3 and anti-DPP10 antibodies specifically detect their respective target proteins. The antibodies were checked by probing immunoblots with extracts from oocytes with or without Kv4.2, KChIP3 or DPP10 cRNA injection. *B*, anti-DPP10 and anti-HA antibodies detect the same HA/DPP10 proteins. In addition, the blots also show that neither antibody cross-reacts with Kv4.2 proteins. *C*, Kv4.2 proteins promote the coimmunoprecipitation of DPP10 and KChIP3. Oocytes expressing HA-tagged KChIP3 (HA/KChIP3) and DPP10 with and without Kv4.2

inactivation. In agreement, steady-state inactivation of Kv4.2 + KChIP3 + DPP10 channels showed a significant rightward shift in voltage dependence when compared with that of Kv4.2 + DPP10 channels (midpoint voltage of activation ($V_{0.5}$): Kv4.2 + DPP10 = -74 ± 2 mV, $n = 11$; Kv4.2 + KChIP3 + DPP10 = -68 ± 3 mV, $n = 4$) (Fig. 3*D*).

The combined functional effects of KChIP3 and DPP10 on Kv4.2 channels in CHO cells are similar to those in oocytes

Using whole-cell patch recordings, coexpression studies were also conducted in CHO cells to determine the cell-type specificity of the observed effects and to characterize rapid gating events, such as kinetics of activation. In general, the effects were remarkably consistent between CHO cells and oocytes. CHO cells were cotransfected with Kv4.2, DPP10 and KChIP3 cDNAs at equal molar concentrations. Coexpression of KChIP3 increased the density of Kv4.2 current ~14 times (Kv4.2 = 54 ± 13 pA pF^{-1}, $n = 10$; Kv4.2 + KChIP3 = 783 ± 82 pA pF^{-1}, $n = 5$), whereas DPP10 increased current density by an average of ~7 times (Kv4.2 + DPP10 = 397 ± 92 pA pF^{-1}, $n = 6$). The amount of current increase produced by KChIP3 and DPP10 closely matched previous observations (Kunjilwar *et al.* 2004; Jerng *et al.* 2004*a*; Zagha *et al.* 2005).

As in the oocyte studies, the auxiliary subunits KChIP3 and DPP10, respectively, modified inactivation by markedly slowing or accelerating its time course, and the combined effects of KChIP3 and DPP10 resulted in distinct current kinetics similar to that of Kv4.2 + DPP10 channels (Fig. 4*A*, traces). Half-inactivation times from CHO cell studies were 29.4 ± 2.1 (Kv4.2), 68.2 ± 6.5 (Kv4.2 + KChIP3), $3.2 + 0.2$ (Kv4.2 + DPP10) and 7.2 ± 0.5 ms (Kv4.2 + KChIP3 + DPP10) ($n = 8$, 7, 5 and 8, respectively). Recovery from inactivation was measured at -80 and -100 mV for Kv4.2 and Kv4.2 plus auxiliary subunits in CHO cells using the two-pulse protocol described in the inset. As seen in Fig. 4*A*, channels composed of Kv4 α-subunits alone recovered at -80 mV considerably slower than channel complexes containing Kv4 and auxiliary subunits. In CHO cells, the time constants of recovery from inactivation at -100 mV were 125 ± 9 (Kv4.2), 41 ± 3 (Kv4.2 + KChIP3), 48 ± 4 (Kv4.2 + DPP10), and 18 ± 1 ms (Kv4.2 + KChIP3 + DPP10) ($n = 7$, 8, 4 and 5, respectively). DPP10 and KChIP3 individually accelerated Kv4.2 recovery from inactivation by approximately threefold in both oocytes and CHO cells. When DPP10 and KChIP3 were both assembled with Kv4.2, the channel complex recovered from inactivation at -100 mV, as compared with Kv4.2 alone, which was ~7 times faster in CHO cells as compared with ~10 times faster in oocytes.

Activation kinetics are robustly modulated by the simultaneous association of Kv4 channels with both DPP10 and KChIP3. Although this finding was suggested by two-electrode voltage-clamp recordings on oocytes, it was made more certain by the higher bandwidth offered by whole-cell patch recordings from CHO cells. Figure 4*B* illustrates the rise of +50 mV normalized currents expressed by channels containing Kv4.2 alone, Kv4.2 with either KChIP3 or DPP10, and Kv4.2 with both DPP10 and KChIP3. The Kv4.2 + DPP10 and Kv4.2 + KChIP3 + DPP10 currents both began to rise at a time point significantly earlier than that for Kv4.2 and Kv4.2 + KChIP3 currents, indicating that DPP10 accelerates the activation process in a manner that persists in the presence of KChIP3. Moreover, Kv4.2 + DPP10 and Kv4.2 + KChIP3 + DPP10 currents exhibited matching kinetics and significantly decreased time-to-peak values at all voltages tested (Fig. 4*B* and *C*).

Ternary complex formation attenuates the influence of cellular environment on channel properties

The properties of currents mediated by just Kv4.2 proteins reportedly vary with cell type, which is likely to be a result of different cellular environments (Petersen & Nerbonne, 1999). Most prominently, the time courses of inactivation and recovery from inactivation are significantly faster in mammalian cells than in *Xenopus* oocytes. Indeed, we observed that currents expressed by Kv4.2 alone decayed more quickly in CHO cells than oocytes, and multiexponential fittings indicated a greater contribution of the dominant fast component ($\tau = 19$ ms) to macroscopic Kv4.2 inactivation in CHO cells (%: oocyte = 54 ± 2, $n = 25$; CHO = 74 ± 3, $n = 9$).

(as indicated) were treated with a reversible cross-linking reagent and solubilized. Goat (cntrl) IgG, anti-HA and anti-Kv4.2 antibodies were added to the extracts, and the immunoprecipitants were recovered by protein A/G Sepharose beads, denatured by SDS, and reduced by dithiothreitol. Immunoprecipitated proteins on Western blots were probed with anti-DPP10 (*a*), anti-KChIP3 (*b*), anti-Kv4.2, (*c*) and anti-HA antibodies (*d*). Samples of the starting extract (extract) are also provided for comparison. *D*, the coimmunoprecipitation of KChIP3 with DPP10 was made possible by the presence of Kv4.2 proteins. Oocytes expressing HA-tagged DPP10 (HA/DPP10) and KChIP3 with and without Kv4.2 were processed for immunoprecipitation in the same way as described earlier. Arrowheads point to the expected molecular masses of respective proteins, and arrows indicate the protein bands that show DPP10 and KChIP3 coimmunoprecipitate in the presence of Kv4.2, revealing the three-protein complex.

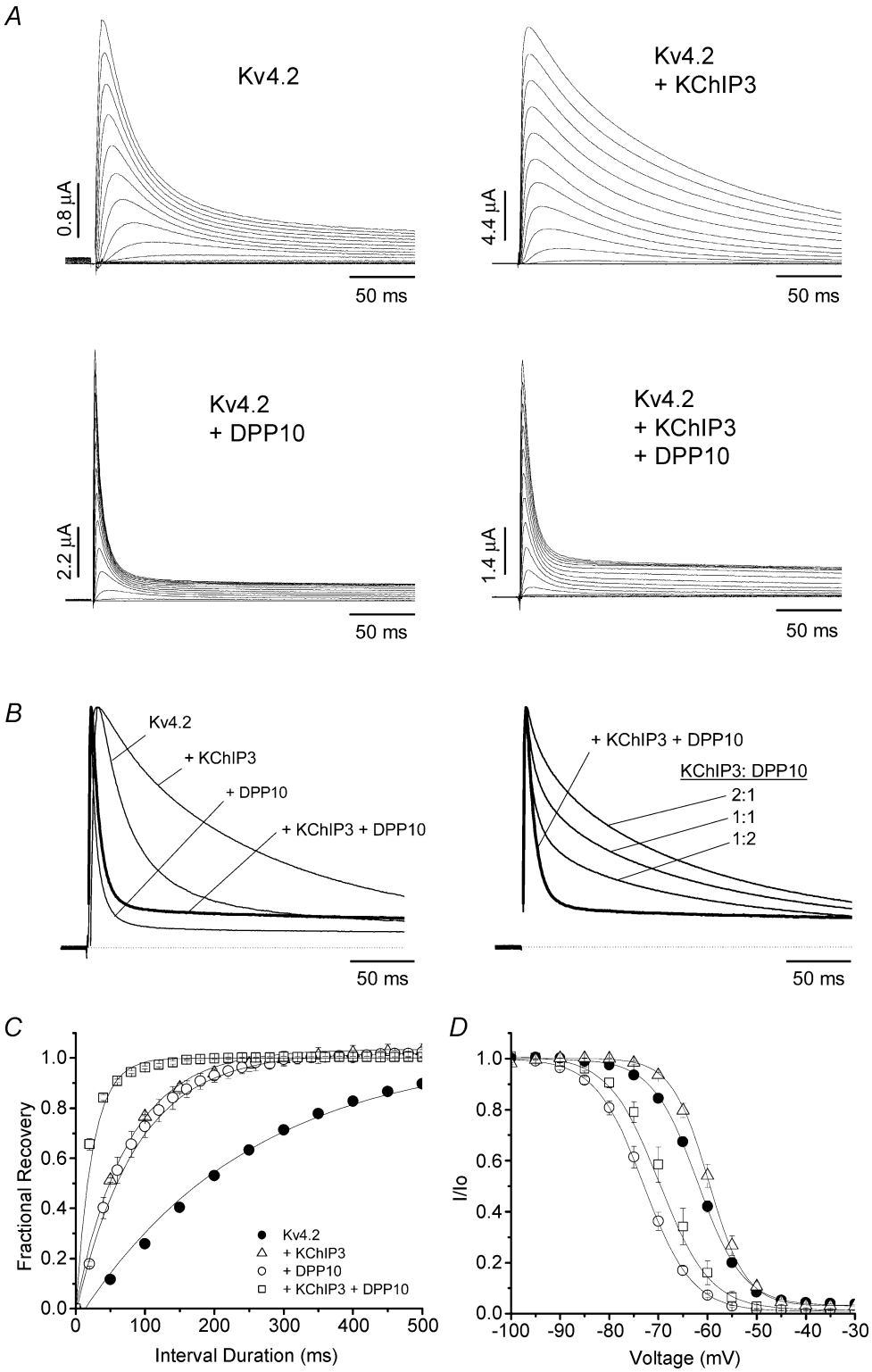

Figure 3. Ternary complex formation of Kv4.2, DPP10 and KChIP3 in oocytes results in currents with inactivation faster than Kv4.2 alone and distinct from those of Kv4.2 + DPP10 and Kv4.2 + KChIP3 binary complexes: kinetics of inactivation and recovery from inactivation

A, families of current traces elicited by step depolarizations from −100 to +50 mV for 1 s using two-electrode voltage clamp. Only the first 250 ms is shown. *B*, normalized and overlapped traces at +50 mV (left), and traces based on arithmetic sums of Kv4.2 + KChIP3 and Kv4.2 + DPP10 currents superimposed with that of the actual Kv4.2 + KChIP3 + DPP10 (bold traces) recording (right). *C*, time course of recovery from inactivation at −100 mV,

The difference in inactivation kinetics was not detected ($P > 0.1$) using $t_{0.5}$ measurements, because in both cases the fastest component constituted more than 50% of the total decay (Fig. 5*A*). Composite data from oocyte and CHO cell experiments are represented in Fig. 5 by open and filled bars/symbols, respectively. Our results confirm that Kv4.2 channels recover from inactivation dramatically faster in CHO cells as compared with oocytes (Fig. 5*B*). In addition, the conductance–voltage relationships of Kv4.2 channels differed significantly depending on expression system. The half-inactivation voltage ($V_{0.5}$) in oocytes occured at ~13 mV more positive than in CHO cells, and the slope of the Boltzmann fit in oocytes was ~2.6 times more shallow (Fig. 5*C*). The midpoint voltage of steady-state inactivation of Kv4.2 channels did not differ between oocyte and CHO cells ($P > 0.25$), while the corresponding slope factor in oocyte was 71% of that in CHO cells (Fig. 5*D*).

In general, coexpression of Kv4.2 with KChIP3 or DPP10 maintained the relative differences between the biophysical properties observed in the two expression systems (Fig. 5). However, many biophysical parameters showed less dispersion in channels incorporating both KChIP3 and DPP10/DPP6 auxiliary proteins, with the exception of a larger shift in the $V_{0.5}$. For example, Kv4.2 + KChIP3 + DPP10 currents from these expression systems varied slightly in their $t_{0.5}$ values (Fig. 5*A*) and were statistically indistinguishable in their τ_{rec} values (Fig. 5*B*, $P > 0.125$), $V_{0.5}$ of the conductance–voltage relationship (Fig. 5*C*, $P > 0.10$), and k of steady-state inactivation (Fig. 5*D*, $P > 0.4$). This suggests that discrepancies in Kv4 properties from different heterologous systems may in part be attributed to the influence of environmental factors on sites normally controlled in a dominant manner by auxiliary subunits.

DPP10 and DPP6 confer dramatically different inactivation to the Kv4 macromolecular complex

Nadal *et al.* (2003) reported that oocytes coinjected with Kv4.2, KChIP1 and DPP6-S have A-type K^+ currents that recover from inactivation at −110 mV with a time course comparable to that from oocytes coinjected with Kv4.2 and DPP6-S. This result differs from our studies using DPP10 and KChIP3, where we found that coexpression produced a further enhancement in recovery kinetics (see Fig. 3*C*). We were therefore interested in comparing the functional properties of channels composed of Kv4.2, KChIP3 and DPP6 to those with Kv4.2, KChIP3 and DPP10. Whole-cell patch recordings were conducted on CHO cells transfected with Kv4.2 cDNA alone or with various combinations of KChIP3 and DPP6 cDNAs. Figure 6*A* shows families of current traces elicited by step membrane depolarizations of CHO cells transfected with Kv4.2 and DPP6-S cDNAs at a 1:1 molar ratio. Compared with Kv4.2 + DPP10 currents, the Kv4.2 + DPP6-S currents inactivated markedly slower, as reported previously from oocyte experiments (see $t_{0.5}$ values in Fig. 5*A*; Jerng *et al.* 2004*a*). The Kv4.2 + DPP6-S currents in CHO cells at +50 mV appeared to differ from Kv4.2 currents mainly in their time-to-peak current, and not in their inactivation time course (Fig. 6*E*). This result differs from coexpression studies in oocytes, where DPP6-S significantly accelerates the overall time course of inactivation (Nadal *et al.* 2003; Jerng *et al.* 2004*a*).

The paucity of the DPP6-S effect on Kv4.2 current decay in CHO cells is further illustrated in Fig. 6*B*, where the addition of KChIP3 markedly slows the time course of inactivation. At +50 mV, the Kv4.2 + KChIP3 + DPP6-S currents resulting from cDNA cotransfection at 1:1:1 molar ratios exhibited waveforms that resembled those of Kv4.2 + KChIP3 (Fig. 6*E*). The half-inactivation times for Kv4.2 + KChIP3 + DPP6-S and Kv4.2 + KChIP3 channels in CHO cells were 61.3 ± 1.5 ($n = 4$) and 68.2 ± 6.5 ms ($n = 7$), which are statistically not distinguishable (Fig. 5*A*; $P > 0.25$). The Kv4.2 + KChIP3 + DPP6-S currents did not match the predicted current waveforms for arithmetic sums of Kv4.2 + KChIP3 and Kv4.2 + DPP6-S at various ratios, indicating that coexpression of KChIP3 and DPP6-S with Kv4.2 does not result in two distinct populations of binary channel complexes (Fig. 6*F*). Note the distinct rounded initial phase of current decay in the Kv4.2 + KChIP3 + DPP6-S trace and its absence in the summed traces. In addition, the same results were obtained with Kv4.2 complexed with DPP6-L (long variant) and KChIP3, indicating the effect is not restricted to the DPP6-S splice form (Fig. 6*C* and *D*).

In contrast to these results in CHO cells, in oocytes, the Kv4.2 + KChIP3 + DPP6-S currents decayed significantly faster than those of Kv4.2 + KChIP3, as indicated by their respective $t_{0.5}$ values (Fig. 5*A*; $P > 0.005$). The difference in inactivation is unlikely to be due to an insufficient expression of an auxiliary subunit component (such as DPP6) in CHO cells, since coexpression

as measured by the two-pulse protocol. Channels were held at −100 mV before they were subjected to double depolarizing pulses to +50 mV with variable time intervals at −100 mV. Data were described by single-exponential fits. *D*, steady-state inactivation curves for various experiments (key shown in *C*). Current availability at indicated voltages was determined at +50 mV following a 10 s conditioning pulse. The lines represent curve fittings using the Boltzmann equation.

of Kv4.2, KChIP3 and DPP6-L at 1:0.1:1 and 1:1:1 molar ratios produces the same functional effects (K. Kunjilwar, unpublished observations). Instead, this finding is consistent with a more robust effect of DPP6 on channel inactivation in oocytes. Interestingly, the resulting Kv4.2 + KChIP3 + DPP6-S currents in oocytes inactivated with $t_{0.5}$ values matching those from CHO cells ($P > 0.10$) (Fig. 5*A*).

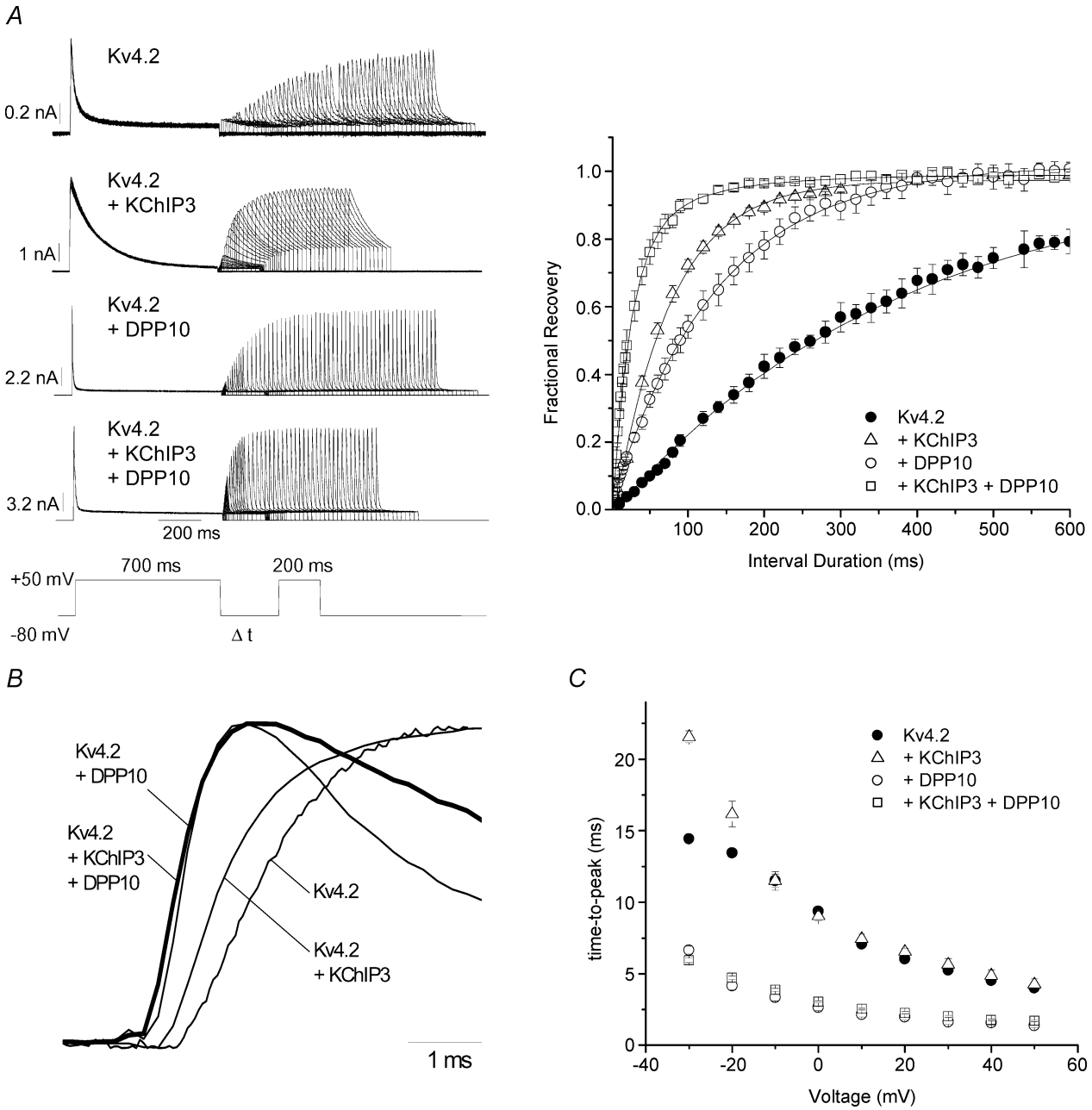

Figure 4. Accelerated kinetics of activation and recovery from inactivation of Kv4.2 + KChIP3 + DPP10 channels heterologously expressed in CHO cells

A, recovery from inactivation at −80 mV. Left, current traces evoked at +50 mV by a two-pulse protocol, as described in the inset. Right, mean fractional recovery from inactivation at −80 mV plotted against interval duration for Kv4.2 with and without auxiliary subunits (Kv4.2, $n = 5$; Kv4.2 + DPP10, $n = 6$; Kv4.2 + KChIP3, $n = 6$; Kv4.2 + KChIP3 + DPP10, $n = 7$). The peak current of the second pulse was normalized against that of the first pulse, and the recovery was fitted with a single-exponential function to yield time constants. *B*, normalized rising phase of representative +50 mV currents from cells expressing Kv4.2, Kv4.2 + DPP10, Kv4.2 + KChIP3 and Kv4.2 + KChIP3 + DPP10 (bold trace), as indicated. Note that Kv4.2 + DPP10 and Kv4.2 + KChIP3 + DPP10 currents began their ascensions significantly earlier than Kv4.2 and Kv4.2 + KChIP3 currents. *C*, the voltage dependence of time-to-peak current for Kv4.2 plus auxiliary subunits.

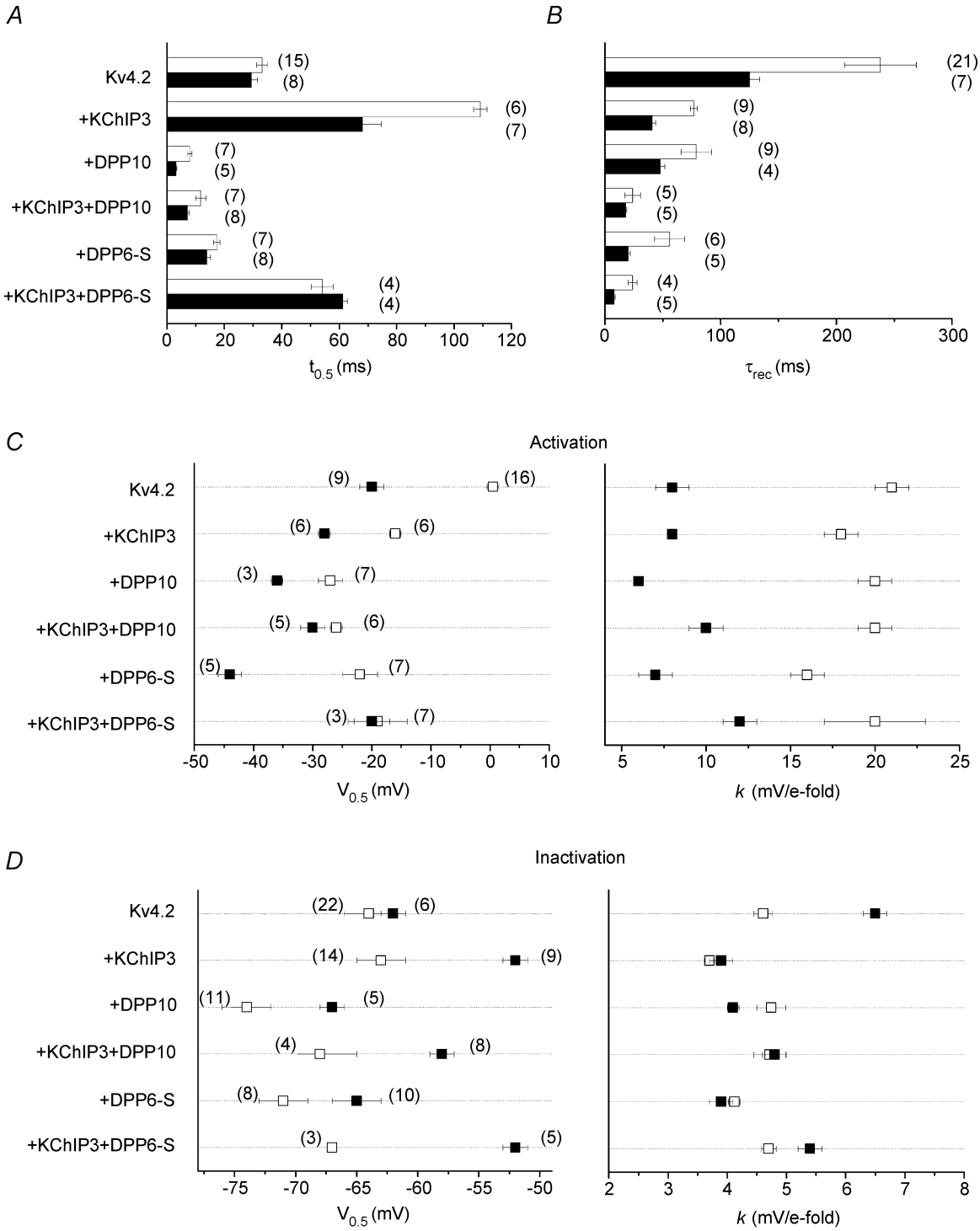

Figure 5. Comparison of time- and voltage-dependent properties of Kv4.2-mediated currents in *Xenopus* oocytes and CHO cells

Open symbols, oocyte data; filled symbols, Chinese hamster ovary (CHO) cell data. *A*, development of macroscopic inactivation at +50 mV assessed by the time when the current reaches half of maximum value ($t_{0.5}$). *B*, kinetics of recovery from inactivation at −100 mV, indicated by time constants (τ_{rec}) of monoexponential curve fittings. *C*, voltage dependence of steady-state activation. The half-activation voltage ($V_{0.5}$) and slope factor (k) were derived from curve fittings using a first-order Boltzmann function. *D*, voltage dependence of steady-state inactivation, described by $V_{0.5}$ and k parameters of first-order Boltzmann functions. Values are presented as means ± S.E.M., with the number of samples shown in parentheses. $V_{0.5}$ and k parameters share the same n.

Despite differences in inactivation kinetics, Kv4 + DPL + KChIP3 ternary complexes containing either DPP10 or DPP6 exhibit recovery from inactivation faster than those of binary complexes

Even though Kv4.2 + KChIP3 + DPP6-S and Kv4.2 + KChIP3 + DPP10 channels inactivated very differently under strong depolarizations, both ternary channel complexes recovered from inactivation dramatically more rapidly than their particular binary complexes (Figs. 4*A* and 7*A*). Figure 7*A* shows currents recorded using a two-pulse protocol, from CHO cells expressing Kv4.2 and DPP6-S (upper traces) *versus* those expressing Kv4.2, DPP6-S and KChIP3

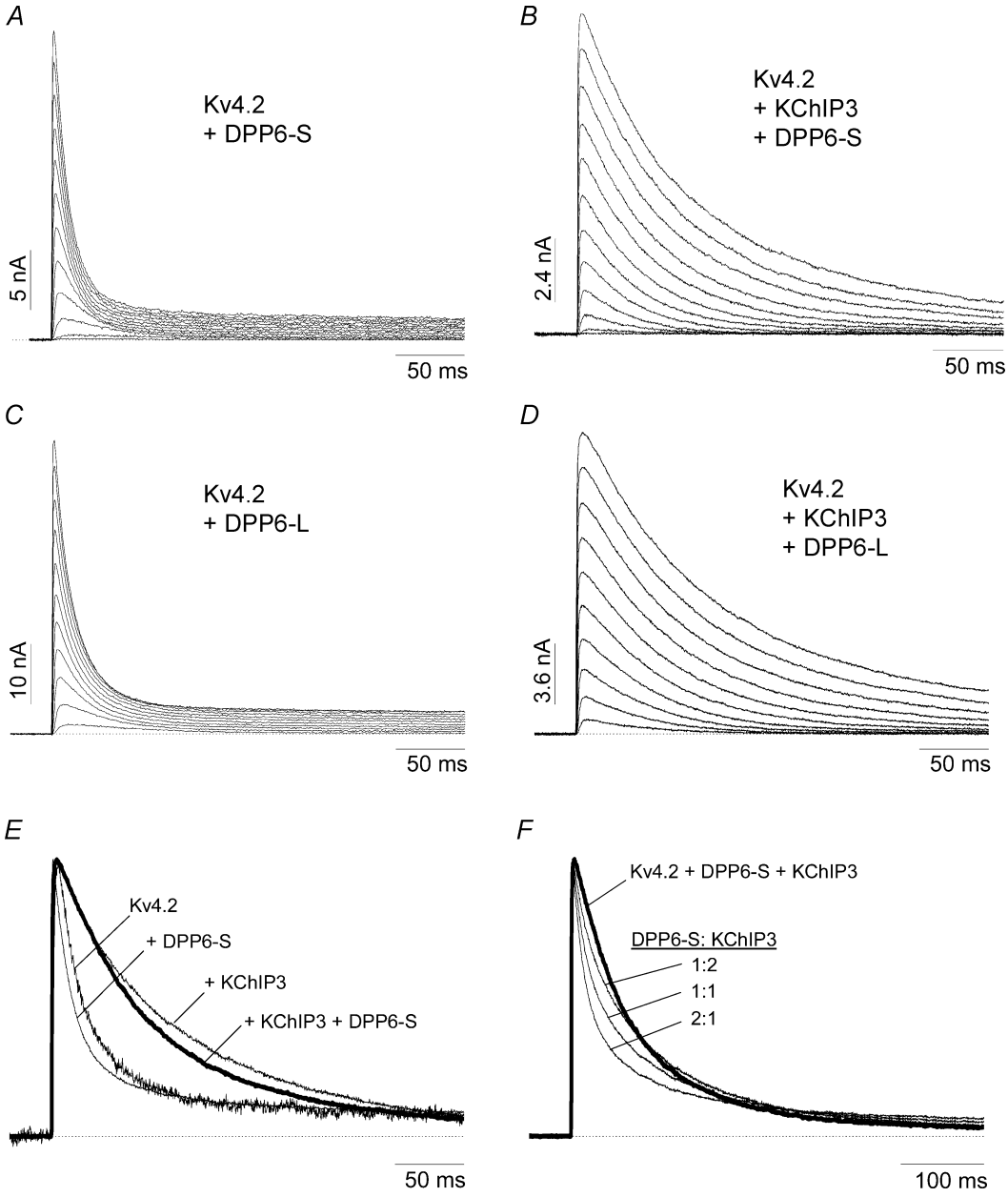

Figure 6. Inactivation of the Kv4.2 + KChIP3 + DPP6 complex channel is dramatically slower than that of the Kv4.2 + KChIP3 + DPP10 channel, reflecting differing modulation of Kv4.2 inactivation by the two DPL variants

A–D, representative current traces of Kv4.2 + DPP6-S (*A*), Kv4.2 + KChIP3 + DPP6-S (*B*), Kv4.2 + DPP6-L (*C*), and Kv4.2 + KChIP3 + DPP6-L (*D*) elicited by voltage steps from a potential of −100 mV to voltages between −60 and +50 mV in 10 mV increments. Note that, despite having markedly different cytoplasmic N-terminal domains, DPP6-S and DPP6-L have nearly identical effects on Kv4.2 current waveform in the absence or presence of KChIP3. *E*, normalized and superimposed traces of Kv4.2 at +50 mV, with and without the indicated auxiliary subunits. The Kv4.2 + KChIP3 + DPP6-S trace is shown with a bold line. *F*, Kv4.2 + KChIP3 + DPP6-S current does not match the arithmetic sum of Kv4.2 + DPP6-S and Kv4.2 + KChIP3 currents at various percentages of contribution. All currents are of 500 ms in duration, and the dotted line represents zero current.

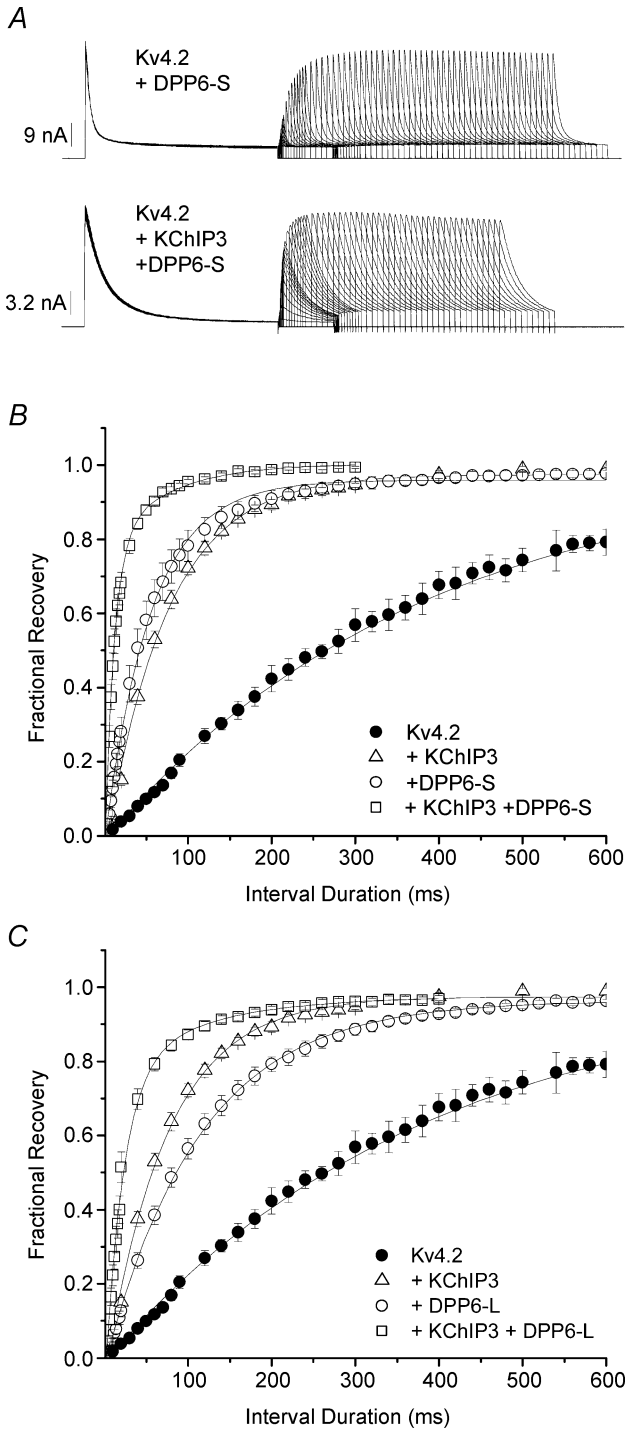

Figure 7. Acceleration of recovery from inactivation attributed to DPP6, like that of DPP10, provides a further boost to the acceleration conferred by KChIP3

A, currents elicited by +50 mV depolarizations during the two-pulse recovery protocol described in Fig. 4. Shown are current traces for Kv4.2 + DPP6-S and Kv4.2 + KChIP3 + DPP6-S channels. Traces for Kv4.2 and Kv4.2 + KChIP3 currents are shown in Fig. 4. *B* and *C*, fractional recovery from inactivation plotted against interpulse interval duration for experiments involving DPP6-S (*B*) and DPP6-L (*C*). Note that for both DPP6-S and DPP6-L, combined effects of DPP6 and KChIP3 on the time course of recovery from inactivation surpass that of either DPP6 or KChIP3 alone. The fractional recovery was fitted with single-exponential functions to provide time constants for comparison. Summary data are plotted in Fig. 5.

(lower traces). The time courses of recovery from inactivation at −80 mV, plotted for current expressed by Kv4.2, Kv4.2 + KChIP3, Kv4.2 + DPP6-S and Kv4.2 + KChIP3 + DPP6-S channels, were best described by monoexponential functions with time constants of approximately 356, 76, 57 and 15 ms, respectively. The summary results for recovery from inactivation at −80 mV are shown in Fig. 7*B* and *C* for channel complexes containing DPP6-S and DPP6-L, respectively. As with DPP10, the addition of DPP6-S or DPP6-L to the Kv4.2 + KChIP3 complex provided a significant boost in the kinetics of recovery from inactivation. This finding, along with the nonadditivity of current decay and other gating parameters, is consistent with the formation of a Kv4.2 + KChIP3 + DPP6 ternary complex.

Different voltage dependence of inactivation accounts for the discrepancy between the inactivations of Kv4.2 + KChIP3 + DPP10 and Kv4.2 + KChIP3 + DPP6 channel complexes

To further investigate the kinetic differences in inactivation associated with DPP10 and DPP6, we normalized and compared traces of Kv4.2 + KChIP3 + DPP10 and Kv4.2 + KChIP3 + DPP6-S currents at −40, 0 and +50 mV (Fig. 8*A*). At −40 mV, the two traces were quite similar, with the Kv4.2 + KChIP3 + DPP6-S current inactivating slightly faster. As the voltage was increased to 0 and +50 mV, the Kv4.2 + KChIP3 + DPP10 inactivated faster, while Kv4.2 + KChIP3 + DPP6-S current decayed markedly slower.

For detailed kinetic quantification, the time courses of inactivation for both channel complexes were fit using the sum of exponential terms. Inactivation of Kv4 channels formed from α-subunits alone has a complex time course well described by the sum of three exponential components (Jerng & Covarrubias, 1997; Bähring *et al.* 2001*b*). Similarly, three exponential terms were necessary for a best fit of Kv4.2 + KChIP3 + DPP10 inactivation, with time constants and fractional amplitudes illustrated in Fig. 8*B* and *C*. We observed that two exponential terms were sufficient to adequately describe Kv4.2 + KChIP3 + DPP6-S inactivation from both oocytes and CHO cells (Fig. 8*D* and *E*). This result is consistent with the findings of Beck *et al.* (2002), which showed that, in the presence of KChIP1, Kv4.1 and Kv4.3, currents in oocytes decay with a biexponential time course.

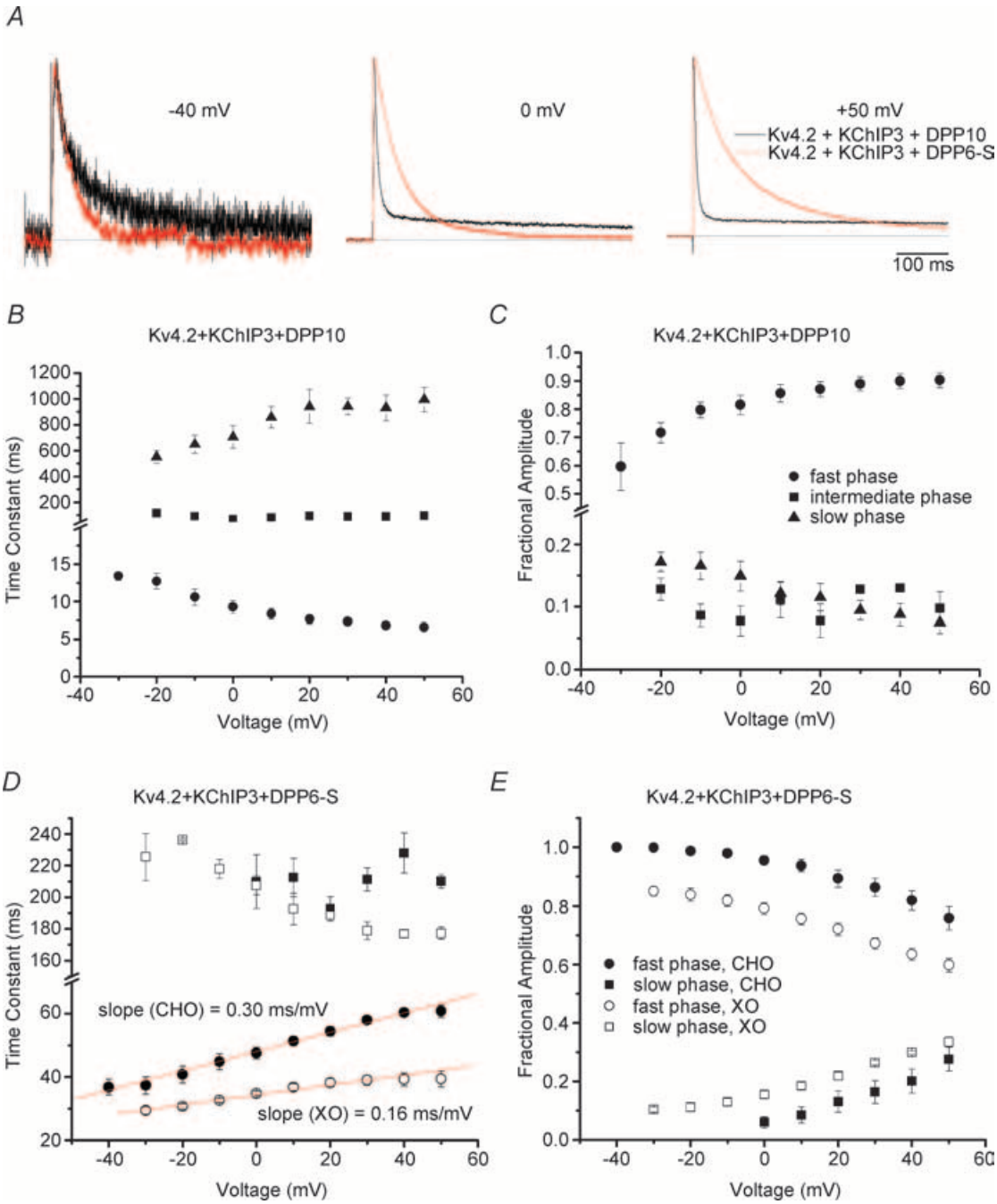

Figure 8. Different voltage dependence of inactivation of Kv4.2 + KChIP3 + DPP10 and Kv4.2 + KChIP3 + DPP6-S channels underlies the dramatic difference in their current decays at more depolarized potentials

A, normalized and overlapped traces of Kv4.2 + KChIP3 + DPP10 (black) and Kv4.2 + KChIP3 + DPP6-S (red) currents at −40, 0 and +50 mV. The depolarizations were of 500 ms duration. Note the increasing disparity between the two traces with increasing membrane potential. *B*, voltage dependence of the fast, intermediate and slow time constants of inactivation for Kv4.2 + KChIP3 + DPP10 currents. Note that inactivation of the fast phase accelerates with increasing voltage. *C*, voltage dependence for the fractional contributions of the fast, intermediate and slow inactivating components. The fast component occupies an increasing percentage as voltage increases, leading to increasing faster overall inactivation with depolarization. The intermediate and slow inactivating components each contribute to ∼10% of total macroscopic inactivation. *D*, voltage dependence of the fast and slow time constants of inactivation for Kv4.2 + KChIP3 + DPP6-S channels in CHO cells (●) and *Xenopus* oocytes (○). Inactivation of the fast phase from both expression systems slows with increasing voltage. Linear fitting of the fast time constants reveals differing voltage sensitivities (CHO, 0.30 ms mV^{-1}; oocyte, 0.16 ms mV^{-1}). *E*, voltage dependence of fractional amplitudes of the fast and slow inactivating components. Contribution from the fast component decreased with voltage.

In evaluating the voltage dependence of inactivation kinetics, we focused our attention on the fast phase that overwhelmingly dominated inactivation in both channels in CHO cells (at +50 mV: Kv4.2 + KChIP3 + DPP10 = 90 ± 3%, $n = 8$; Kv4.2 + KChIP3 + DPP6-S = 75.8 ± 4%, $n = 5$) (Fig. 8*C* and *E*). As Fig. 8*B* shows, the time constant of the fast phase for Kv4.2 + KChIP3 + DPP10 channels slightly decreased with positive membrane depolarization (Fig. 8*B*). Meanwhile, the faster time constant notably increased with voltage for Kv4.2 + KChIP3 + DPP6-S channels, with a slope of ∼0.3 ms mV^{-1}. The same effects were observed in both oocyte and CHO cell recordings (Fig. 8*D* and *E*). Our measurements of the inactivation of the channel in oocyte also detected slowing of inactivation with increasing voltage, but at only approximately half of the voltage sensitivity (slope = 0.15 ms mV^{-1}) (Fig. 8*D*). Furthermore, differences were observed in the contribution of the fast inactivating phase as a function of voltage. The fractional amplitude of the fast dominant phase increased and decreased with depolarization in Kv4.2 + KChIP3 + DPP10 and Kv4.2 + KChIP3 + DPP6-S channels, respectively (Fig. 8*C* and *E*).

Discussion

We have determined that KChIP3 and DPP10 can simultaneously coassemble with Kv4.2 α-subunits to form a multiprotein channel complex. The Kv4.2 + KChIP3 + DPP10 ternary complex functionally behaves like many native subthreshold A-type channels, prominently characterized by rapid inactivation and recovery from inactivation. The precise calibration of Kv4 channel properties, including activation, inactivation and recovery, is important for channel function in the regulation of firing frequency, backpropagating action potentials, and dendritic signal integrations. We have also demonstrated that, within the Kv4.2 + KChIP3 + DPL macromolecular complex, the dipeptidyl-peptidase-like subunits (i.e. DPP10 and DPP6) influence the time course of inactivation at positive membrane potentials. The differential effects of DPP10 and DPP6 mainly result from contrasting dependence of inactivation kinetics on voltage.

DPP10 and KChIP3 coexist in the same Kv4 channel complex

Previously, it has been suggested that some of the Kv4 complexes from rat cerebellum may contain both DPP6 and KChIPs (Nadal *et al.* 2003), and we have now demonstrated the ternary complex containing DPP10 and KChIP3 in rat cortex, and shown that heterologously expressed DPP10 and KChIP3 coassemble with Kv4 proteins to produce a channel complex with distinct novel functional properties. Ternary complex formation presents an increased level of I_{SA} molecular complexity that may underlie functional diversity in neurones. At present, there reportedly exists three subfamily members of Kv4 genes (Kv4.1, Kv4.2 and Kv4.3), with the Kv4.3 gene having both long and short C-terminal splice variants (Kv4.3L and Kv4.3S) (reviewed by Jerng *et al.* 2004*b*). Four subfamilies of KChIPs have been identified, many with their own N-terminal splice variants (KChIP1a–b, KChIP2a–d, KChIP3, KChIP4a–b). DPP6 has both long and short N-terminal variants (DPP6-S and DPP6-L), and a new N-terminal variant has recently been discovered for DPP10. By calculation, in the absence of heterogeneous mixing of variant subunits, 144 different Kv4 + DPL + KChIP complexes are possible (4 Kv4 × 9 KChIPs × 4 DPL). If the potential mixing of different Kv4, DPL and KChIP subunits is taken into account, the number of possible channels with distinct subunit compositions is far greater. However, the number of actual combinations of Kv4 α and auxiliary subunits may be restricted by their specific tissue- or population-specific expressions (Table 1), and not all combinations necessarily lead to distinct functional behaviours. For example, association of Kv4.1 and Kv4.3 with KChIP1 results in channels with similar kinetic and voltage-dependent properties (Beck *et al.* 2002).

Our heterologous coexpression studies show that either KChIP3 or DPP10 is sufficient and capable in facilitating maximal Kv4 surface expression, as their coexpression does not result in additional current. Currently, it is unclear whether the native expression of subthreshold A-type channels in neurones is sensitive to the loss of either auxiliary subunit. KChIP3 and KChIP2 are selectively expressed at approximately equal levels in dentate gyrus of hippocampus (Table 1), and knocking out KChIP3 expression in mice leads to a moderate decrease in the transient A-type current from dentate gyrus granule cells (Lilliehook *et al.* 2003). The remaining current expressed may be attributed to Kv4 channels associated with KChIP2 and/or DPP6. Further experiments will be needed to unravel the roles of KChIPs and DPLs in the native expression of Kv4 ternary complex.

The Kv4.2 + KChIP3 + DPP10 current expressed in heterologous systems exhibits biophysical properties matching those of neuronal I_{SA}

How do the biophysical properties of Kv4.2 + KChIP3 + DPP10 channels compare with those of neuronal subthreshold A-type channnels? The voltage dependence and voltage sensitivity of steady-state activation and inactivation of the ternary complex channel are in line

with the reported values for neuronal subthreshold A-type channels, which exhibit significant variability (Jerng *et al.* 2004*b*). Most importantly, our study demonstrates that A-type channels consisting of Kv4.2, KChIP3 and DPP10 express surprisingly fast kinetics of activation, inactivation, and recovery from inactivation, which are features fundamental to neuronal subthreshold A-type channel functions. In comparison with published results, both kinetic parameters of native subthreshold A-type channels are reproduced by Kv4.2 + KChIP3 + DPP10 channels expressed in heterologous cells (Fig. 9). In particular, inactivation of Kv4.2 + KChIP3 + DPP10 in CHO cells and oocytes more closely matches those of subthreshold A-type channels from cortical pyramidal cells, which are neurones that express more DPP10 than DPP6 overall (Table 1). The current recorded from cortical pyramidal cells from layers 2, 5 and 6 inactivated mono-exponentially with a time constant of 7–12 ms, which matches those of the fast phase that dominate inactivation of Kv4.2 + KChIP3 + DPP10 in CHO cells and oocytes (Fig. 8*B*; Banks *et al.* 1996; Bekkers, 2000; Korngreen & Sakmann, 2000; Dong & White, 2003).

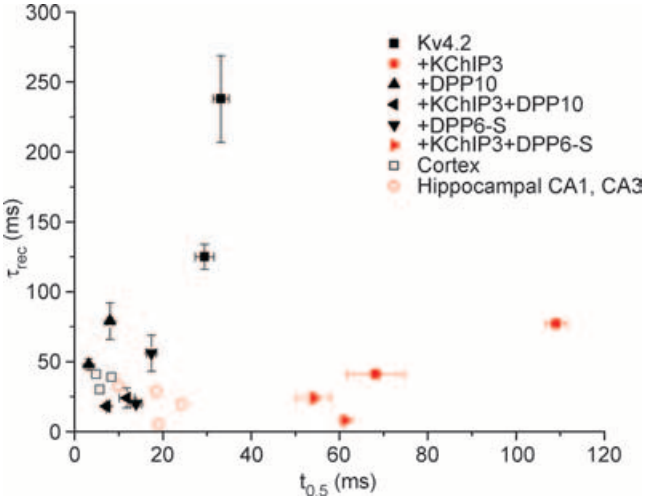

Figure 9. Modulated simultaneously by KChIP3 and DPP10, Kv4.2-mediated current inactivates and recovers from inactivation like native subthreshold A-type current (I_{SA})
Data from heterologous expression systems are compared with those of native cells, with half-inactivation times ($t_{0.5}$, at +50 mV) plotted against respective recovery time constants (τ_{rec}, at −100 mV) (refer to Fig. 7 for oocyte and CHO cell values). Half-inactivation times are between +30 and +50 mV; recovery data are between −100 and −120 mV. Recovery time constants from Johnston *et al.* (2000) and Martina *et al.* (1998) were derived by plotting and fitting published data with single-exponential functions. Symbols in red indicate currents with inactivation slowing with depolarization. Published rat cortical data: Bekkers (2000); Korngreen & Sakmann (2000); Dong & White (2003). Published rat hippocampal CA1 and CA3 data: Klee *et al.* (1995); Hoffman *et al.* (1997); Martina *et al.* (1998); Johnston *et al.* (2000).

In contrast, Kv4.2 + KChIP3 + DPP6 channels inactivate significantly slower than Kv4.2 + KChIP3 + DPP10 channels, suggesting that neurones expected to have more DPP6 are likely to show slower inactivation as compared with those with more DPP10. Consistent with the hypothesis, rat hippocampal CA1 and CA3 neurones express significantly more DPP6 and have I_{SA} with inactivation (τ = 15–35 ms) slower than that of cortical neurones (Fig. 9). Yet, as Fig. 9 shows, a marked difference (~40 ms in $t_{0.5}$ values) exists between the inactivation kinetics of Kv4.2 + KChIP3 + DPP6 channels in heterologous systems and that of hippocampal neuronal I_{SA}. Several possible reasons can be suggested, including differences in subunit composition, post-translational modification, and cellular environments. Although the native I_{SA} channel is likely to be based on heterotetramers of α-subunits, since hippocampal neurones express both Kv4.2 and Kv4.3, heterotetramerization is unlikely a contributor, since Kv4.2/Kv4.3 heterotetramers expressed in HEK 293 cells and myocytes do not inactivate faster than Kv4.2 or Kv4.3 homotetramers (Guo *et al.* 2002). Since KChIP3 expression is low in the hippocampus outside of the dentate gyrus, it is more likely that the difference between inactivation kinetics is due to coassembly with other KChIP variants, such as KChIP2 and KChIP4 (Table 1).

The KChIP component may play a modulatory role in the ternary complex channel

In a previous study, the biophysical properties of Kv4.2 + KChIP1 + DPP6-S were characterized in oocytes using two-electrode voltage clamp (Nadal *et al.* 2003). Most interestingly, the Kv4.2 + KChIP1 + DPP6-S channels reportedly inactivate nearly as quickly as the Kv4.2 + DPP6-S channels, and the kinetics of their recovery at −110 mV (τ = 57 ms) are not significantly faster than those of Kv4.2 + KChIP1 (τ = 59 ms) or Kv4.2 + DPP6-S channels (τ = 41 ms) (Nadal *et al.* 2003). These results differed from our findings with Kv4.2 + KChIP3 + DPP6-S channels, which inactivate markedly slower than Kv4.2 + DPP6 S channels and recover with a dramatically faster time course when compared with Kv4.2 + KChIP3 or Kv4.2 + DPP6-S (Figs 5 and 6).

The source of these differences may be due to differential modulation of Kv4.2 by KChIP1 and KChIP3. KChIP3 accelerates Kv4.2 recovery from inactivation by threefold (Fig. 7*B*); KChIP1 accelerates it by twofold (Boland *et al.* 2003; Van Hoorick *et al.* 2003). In addition, Kv4.2 + KChIP1 current inactivates faster than Kv4.2 + KChIP3 current. Kv4.2 + KChIP1 current at +40 mV decays to half-maximum value at ~54 ms (Nadal *et al.* 2003), whereas the half-inactivation time for

Kv4.2 + KChIP3 current at +50 mV is ~109 ms (Fig. 7*A*). A similar difference in modulation of inactivation at low voltage is observed, as KChIP1 accelerates inactivation of Kv4.2 channels at low voltages by 1.8-fold (Boland *et al.* 2003), while KChIP3 apparently has no effect (at −50 mV: τ (wild-type) = 700 ms (Boland *et al.* 2003), τ (+KChIP3) = 700 ms (Kunjilwar *et al.* 2004)). Consequently, the Kv4.2 + KChIP1 + DPP6-S complex has no added acceleration of recovery from inactivation and exhibits inactivation at depolarized potentials faster than Kv4.2 + KChIP3 + DPP6-S.

The contribution of the KChIP subunit component to the functional properties of the native ternary complex is highlighted by a recent study that correlates slower kinetics of I_{SA} in some neurones with cell-specific expression of the KChIP4a variant (Baranauskas, 2004). I_{SA} from globus pallidus (GP) and basal forebrain (BF) neurones in rats have slower inactivation ($\tau > 80$ ms) and deactivation than those from striatal cholinergic interneurones (Strl) and hippocampal area CA1 pyramidal neurones (HIP), and this corresponds with the presence of KChIP4a transcripts in GP and BF neurones and not in Strl and HIP neurones. Since GP neurones also express DPP6 and DPP10 (Zagha *et al.* 2005), the observed slower inactivation suggests that KChIP4a may strongly contribute to the inactivation kinetics of Kv4 + DPL + KChIP4a channels. In agreement, preliminary data from our laboratory show that KChIP4a dramatically slows the inactivation of Kv4.2 + DPP6-S channels in *Xenopus* oocytes (H. H. Jerng, unpublished observations). These data suggest that the KChIP constituent of the native Kv4 complex also has an important role in channel kinetic properties, and the identities of both the KChIP and DPL present will be likely to contribute to the population specificity of I_{SA} properties.

The Kv4.2 + KChIP3 + DPP6 current expressed in CHO cells and oocytes shows slowing of inactivation with membrane depolarization, resembling certain I_{SA}

Interestingly, several reports have stated that the I_{SA} from rat pyramidal neurones (CA1 and CA3) and interneurones of the hippocampus curiously exhibit an increased time constant of inactivation with increasing voltage (Hoffman *et al.* 1997; Klee *et al.* 1995; Lien *et al.* 2002). In cerebellar granule cells that also express predominently more DPP6 than DPP10, Bardoni and Belluzi (1993) also described slowdown of macroscopic inactivation with voltage, observed as depolarization-dependent increases in contribution of the slow component in biexponential decay. We found a similar phenomenon occurring with Kv4.2 + KChIP3 + DPP6 currents, one that is sufficiently robust to produce inactivation dramatically different from that of Kv4.2 + KChIP3 + DPP10 currents at high depolarizations. Calculated from published data, the slope of voltage dependence of inactivation kinetics of hippocampal I_{SA} was ~0.26 ms mV^{-1} (Hoffman *et al.* 1997; Martina *et al.* 1998) or ~0.16 ms mV^{-1} (Klee *et al.* 1995; Lien *et al.* 2002). These values closely match that of Kv4.2 + KChIP3 + DPP6 in CHO cells (0.3 ms mV^{-1}) and oocytes (0.15 ms mV^{-1}). Furthermore, differences between the voltage dependence of this inverse voltage-inactivation relationship may also contribute to differences observed between Kv4.2 + KChIP3 + DPP6-S inactivation seen between oocytes and CHO cells. Curiously, the sensitivity of Kv4.2 + KChIP3 + DPP6-S fast inactivation to voltage in oocytes is half that in CHO cells, and the voltage sensitivity of the *g*–*V* relationship in oocytes is half that in CHO cells (Fig. 7*D*). These observations are consistent with a mechanism where Kv4 channels preferentially inactivate after channel closure at depolarized potentials (see below). Thus, facilitation of channel activation and opening discourages the establishment of inactivation, associating increased activation with decreased inactivation.

Molecular origins of depolarization-dependent slowing of inactivation: KChIP3, DPP6 and closed-state inactivation

The kinetic and molecular bases underlying Kv4 channel inactivation are beginning to be understood (reviewed by Jerng *et al.* 2004*b*). K^+ channels formed from tetrameric assembly of Kv4 α-subunits alone inactivate by two proposed pathways: pore occlusion of the opened channel by the N-terminal inactivation domain (open-state inactivation) (Gebauer *et al.* 2004), or inactivation of closed channels that are partially activated at low voltages (closed-state inactivation) (Jerng *et al.* 1999; Bähring *et al.* 2001*b*). The blocking particle induces a rapid inactivation that is independent of particle electrostatic charge and moderately accelerated by depolarization (Jerng & Covarrubias, 1997; Gebauer *et al.* 2004). Open-state inactivation is unstable and thus transient in Kv4 channels, and, during prolonged depolarizations, Kv4 channels prefer to close and accumulate in a closed-inactivated state, from which they recover rapidly during hyperpolarizations (Bähring *et al.* 2001*b*). Also referred to as 'V-type' or 'U-type' inactivation, closed-state inactivation is affected by mutations in the inner vestibule and exhibits progressively slower inactivation at depolarized potentials (Klemic *et al.* 1998; Jerng *et al.* 1999).

Channels coassembled from Kv4.2, KChIP3 and DPP6 exhibit slowing of inactivation kinetics at depolarized potentials, consistent with our current understanding of

Kv4 inactivation mechanisms. Without KChIP3, the fast pore-block mechanism masks the slowing of inactivation with increasing voltage associated with closed-state inactivation. The binding of KChIP to the N-terminal inactivation domain abolishes or significantly impairs open-state inactivation in Kv4 channels (reviewed by Jerng *et al.* 2004*b*), and consequently closed-state inactivation is made prominent, leading to the observed inactivation slowing in Kv4.2 + KChIP3 + DPP6-S channels. While preferential closed-state inactivation appears to be a major target of DPL (DPP6 and DPP10)-mediated remodelling (Jerng *et al.* 2004*a*; Rocha *et al.* 2005), it is possible that DPLs also participate in the depolarization-dependent stabilization of the opened channel and retardation of inactivation by leftward shifting the voltage dependence of activation and accelerating channel opening. In addition, since hippocampal I_{SA} and Kv4.2 + KChIP3 + DPP6 currents exhibit slowing of inactivation with depolarization, our data therefore suggest that closed-state inactivation underlies the majority of fast inactivation in I_{SA} in neurones that express mostly DPP6.

The absence of depolarization-dependent slowing of inactivation kinetics in Kv4.2 + KChIP3 + DPP10 channels remains a mystery. Considering the relative acceleration which DPP10 and DPP6 imparts on Kv4.2 closed-state inactivation (Jerng *et al.* 2004*a*), it is conceivable that the differential inactivation at high voltage reflects changes at lower voltages with an altered voltage dependence of inactivation kinetics. However, it is plausible that the cytoplasmic N-terminal domain of DPP10 contains a pore-blocking domain that re-establishes fast inactivation from open state in KChIP-bound channels. First, chimeric studies between DPP10 and DPP6 show that the DPP10 cytoplasmic N-terminal domain underlies the faster inactivation associated with DPP10 modulation (Jerng *et al.* 2004*a*). Second, DPP10 coexpression produces DPP10-mediated fast inactivation to Kv4.2 channels without the endogenous N-terminal inactivation domain (ΔN2–40) (H. H. Jerng, unpublished observations). Unlike DPP10, coexpression of DPP6-S or DPP6-L does not significantly alter ΔN2–40 inactivation, consistent with our differential findings on Kv4.2 + KChIP3 + DPP10 and Kv4.2 + KChIP3 + DPP6 channel inactivation. Third, I_{SA} of neurones expressing both DPP10 and DPP6 equally, including populations from GP and thalamus, do not exhibit inactivation that slows with more positive voltage (Huguenard *et al.* 1991; Tkatch *et al.* 2000). Assuming these I_{SA} channels contain both DPP10 and DPP6 subunits, it suggests that the effect of DPP10 on inactivation is dominant over that of DPP6. Conversely, our examination of the amino acid sequence at the DPP10 N terminus finds no cluster of hydrophobic residues, which is the typical signature of an inactivation particle. Therefore, additional work will be required to elucidate the mechanism by which DPP10 confers faster inactivation to the Kv4 and, by inference, the I_{SA} macromolecular complex.

Physiological relevance of understanding the I_{SA} complex consisting of Kv4, KChIP and DPL

Regions where Kv4.2, KChIPs and DPLs are known to have prominent expression (dentate gyrus, neocortex and piriform cortex) are also areas coincidentally associated with epilepsy. The initiation of epileptic seizures may be induced by increased neuronal excitability that results from decreases in subthreshold A-type channel expression or function. For example, the absence of functional Kv4.2 channels in hippocampal heterotopia is associated with hyperexcitable firing (Castro *et al.* 2001). Hyperpolarized steady-state inactivation of I_{SA} from temporal lobe neurones of epilepsy patients may be responsible for network hyperexcitability and epileptiform discharges (Ruschenschmidt *et al.* 2004). In an animal model of temporal lobe epilepsy, increased dendritic excitability in CA1 pyramidal neurones is linked to a significantly decreased I_{SA} caused by a down-regulation of Kv4.2 channel density and function (Bernard *et al.* 2004). We have shown that KChIPs and DPLs coassemble with Kv4 channels to form subthreshold A-type channels, and they have critical functions in both I_{SA} expression and function. Furthermore, modulation of Kv4.2 gating by phosphorylation can affect channel availability and is dependent on macromolecular complex formation (Schrader *et al.* 2002). Therefore, our understanding of the composition of subthreshold A-type channels is a critical step in deciphering the Kv4-related channelopathies.

References

Allen M, Heinemann A, Noguchi E, Abecasis G, Broxholme J, Ponting CP *et al.* (2003). Positional cloning of a novel gene influencing asthma from Chromosome 2q14. *Nat Genet* **35**, 258–263.

An WF, Bowlby MR, Betty M, Cao J, Ling HP, Mendoza G *et al.* (2000). Modulation of A-type potassium channels by a family of calcium sensors. *Nature* **403**, 553–556.

Bähring R, Boland LM, Varghese A, Gebauer M & Pongs O (2001*b*). Kinetic analysis of open- and closed-state inactivation transition in human Kv4.2 A-type potassium channels. *J Physiol* **535**, 65–81.

Bähring R, Dannenberg J, Peters HC, Leicher T, Pongs O & Isbrandt D (2001*a*). Conserved Kv4 N-terminal domain critical for effects of Kv channel-interacting protein 2.2 on channel expression and gating. *J Biol Chem* **276**, 23888–23894.

Banks MI, Haberly LB & Jackson MB (1996). Layer-specific properties of the transient K^+ current (I_A) in piriform cortex. *J Neurosci* **16**, 3862–3876.

Baranauskas G (2004). Cell-type-specific splicing of KChIP4 mRNA correlates with slower kinetics of A-type current. *Euro J Neurosci* **20**, 385–391.

Bardoni R & Belluzzi O (1993). Kinetic study and numerical reconstruction of A-type current in granule cells of rat cerebellar slices. *J Neurophysiol* **69**, 2222–2231.

Barrett AJ, Rawling ND & O'Brien EA (2001). The MEROPS database as a protease information system. *J Struct Biol* **134**, 95–102.

Baxter DA & Byrne JH (1991). Ionic conductance mechanisms contributing to the electrophysiological properties of neurons. *Curr Opin Neurobiol* **1**, 105–112.

Beck EJ, Bowlby M, An WF, Rhodes KJ & Covarrubias M (2002). Remodeling inactivation gating of Kv4 channels by KChIP1, a small-molecular-weight calcium-binding protein. *J Physiol* **538**, 691–706.

Bekkers JM (2000). Distribution and activation of voltage-gated potassium channels in cell-attached and outside-out patches from large layer 5 cortical pyramidal neurons of the rat. *J Physiol* **525**, 611–620.

Bernard C, Anderson A, Becker A, Poolos NP, Beck H & Johnston D (2004). Acquired dendritic channelopathy in temporal lobe epilepsy. *Science* **305**, 532–535.

Boland LM, Jiang M, Lee SY, Fahrenkrug SC, Harnett MT & O'Grady SM (2003). Functional properties of a brain-specific NH_2-terminally spliced modulator of Kv4 channels. *Am J Physiol Cell Physiol* **285**, C161–170.

Buxbaum JD, Choi EK, Luo Y, Lilliehook C, Crowley AC, Merriam DE *et al.* (1998). Calsenilin: a calcium-binding protein that interacts with the presenilins and regulates the levels of a presenilin fragment. *Nat Med* **4**, 1177–1181.

Carrion AM, Link WA, Ledo F, Mellstrom B & Naranjo JR (1999). DREAM is a Ca^{2+}-regulated transcriptional repressor. *Nature* **398**, 80–84.

Castro PA, Cooper EC, Lowenstein DH, Baraban SC (2001). Hippocampal heterotopia lack functional Kv4.2 potassium channels in the methylazoxymethanol model of cortical malformation and epilepsy. *J Neurosci* **21**, 6626–6634.

Chen T, Ajami K, McCaughan GW, Gorrell MD & Abbott CA (2003). Dipeptidyl peptidase IV gene family. *Adv Exp Med Biol* **524**, 79–86.

Cheng HY, Pitcher GM, Laviolette SR, Whishaw IQ, Tong KI, Kockeritz LK *et al.* (2002). DREAM is a critical transcriptional repressor for pain modulation. *Cell* **108**, 31–43.

Connor JA & Stevens CF (1971). Prediction of repetitive firing behaviour from voltage clamp data on an isolated neurons soma. *J Physiol* **213**, 31–53.

de Lecea L, Soriano E, Criado JR, Steffensen SC, Henriksen SJ & Sutcliffe JG (1994). Transcripts encoding a neural membrane CD26 peptidase-like protein are stimulated by synaptic activity. *Mol Brain Res* **25**, 286–296.

Dong Y & White FJ (2003). Dopamine D1-class receptors selectively modulate a slowly inactivating potassium current in rat medial prefrontal cortex pyramidal neurons. *J Neurosci* **23**, 2686–2695.

Gebauer M, Isbrandt D, Sauter K, Callsen B, Nolting A, Pongs O *et al.* (2004). N-type inactivation features of Kv4.2 channel gating. *Biophys J* **86**, 210–223.

Guo W, Li H, Aimond F, Johns DC, Rhodes KJ, Trimmer JS *et al.* (2002). Role of heteromultimers in the generation of myocardial transient outward K^+ currents. *Circ Res* **90**, 586–593.

Hille B (2001). *Ion Channels of Excitable Membranes*. Sinauer Associates, Sunderland, MA.

Hoffman DA, Magee JC, Colbert CM & Johnston D (1997). K^+ channel regulation of signal propagation in dendrites of hippocampal pyramidal neurons. *Nature* **387**, 869–875.

Holmqvist MH, Cao J, Hernandez-Pineda R, Jacobson MD, Carroll KI, Sung MA *et al.* (2002). Elimination of fast inactivation in Kv4 A-type potassium channels by an auxiliary subunit domain. *Proc Natl Acad Sci U S A* **99**, 1035–1040.

Hough RB, Lengeling A, Bedian V, Lo C & Bucan M (1998). *Rump white* inversion in the mouse disrupts dipeptidyl aminopeptidase-like protein 6 and causes dysregulation of *Kit* expression. *Proc Natl Acad Sci U S A* **95**, 13800–13805.

Huguenard JR, Coulter DA & Prince DA (1991). A fast transient potassium current in thalamic relay neurons: kinetics of activation and inactivation. *J Neurophysiol* **66**, 1304–1315.

Jerng HH & Covarrubias M (1997). K^+ channel inactivation mediated by the concerted action of the cytoplasmic N- and C terminal domains. *Biophys J* **72**, 163–174.

Jerng HH, Pfaffinger PJ & Covarrubias M (2004*b*). Molecular physiology and modulation of somatodendritic A-type potassium channels. *Mol Cell Neurosci* **27**, 343–369.

Jerng HH, Qian Y & Pfaffinger PJ (2004*a*). Modulation of Kv4.2 channel expression and gating by dipeptidyl peptidase 10 (DPP10). *Biophys J* **87**, 2380–2396.

Jerng HH, Shahidullah M & Covarrubias M (1999). Inactivation gating of Kv4 potassium channels: Molecular interactions involving the inner vestibule of the pore. *J Gen Physiol* **113**, 641–659.

Johns DC, Nuss HB & Marban E (1997). Suppression of neuronal and cardiac transient outward currents by viral gene transfer of dominant-negative Kv4.2 constructs. *J Biol Chem* **272**, 31598–31603.

Johnston D, Hoffman DA, Magee JC, Poolos NP, Watanabe S, Colbert CM *et al.* (2000). Dendritic potassium channels in hippocampal pyramidal neurons. *J Physiol* **525**, 75–81.

Kin Y, Misumi Y & Ikehara Y (2001). Biosynthesis and characterization of the brain-specific membrane protein DPPX, a dipeptidyl peptidase IV-related protein. *J Biochem* **129**, 289–295.

Klee R, Ficker E & Heinemann U (1995). Comparison of voltage-dependent potassium currents in rat pyramidal neurons acutely isolated from hippocampal regions CA1 and CA3. *J Neurophysiol* **74**, 1982–1995.

Klemic KG, Shieh CC, Kirsch GE & Jones SW (1998). Inactivation of Kv2.1 potassium channels. *Biophys J* **74**, 1779–1789.

Korngreen A & Sakmann B (2000). Voltage-gated K^+ channels in layer 5 neocortical pyramidal neurones from young rats: subtypes and gradients. *J Physiol* **525**, 621–639.

Kunjilwar K, Strang C, Derubeis D & Pfaffinger PJ (2004). KChIP3 rescues the functional expression of Shal channel tetramerization mutants. *J Biol Chem* **279**, 54542–54551.

Lien C-C, Martina M, Schultz JH, Ehmko H & Jonas P (2002). Gating, modulation, and subunit composition of voltage-gated K^+ channels in dendritic inhibitory interneurones of rat hippocampus. *J Physiol* **538**, 405–419.

Lilliehook C, Bozdagi O, Yao J, Gomez-Ramirez M, Zaidi NF, Wasco W *et al.* (2003). Altered Aβ formation and long-term potentiation in a calsenilin knock-out. *J Neurosci* **23**, 9097–9106.

Malin SA & Nerbonne JM (2000). Elimination of the fast transient in superior cervical ganglion neurons with expression of Kv4.2W362F: Molecular dissection of I_A. *J Neurosci* **20**, 5191–5199.

Martina M, Schultz JH, Ehmke H, Monyer H & Jonas P (1998). Functional and molecular differences between voltage-gated K^+ channels of fast-spiking interneurons and pyramidal neurons of rat hippocampus. *J Neurosci* **18**, 8111–8125.

Nadal MS, Ozaita A, Amarillo Y, Vega-Saenz de Miera E, Ma Y, Mo W *et al.* (2003). The CD26-related dipeptidyl aminopeptidase-like protein DPPX is a critical component of neuronal A-type K^+ channel. *Neuron* **37**, 449–461.

Nagase T, Kikuno R, Ishikawa K, Hirosawa M & Ohara O (2000). Prediction of the coding sequences of unidentified human genes. XVII. The complete sequences of 100 new cDNA clones from brain which code for large proteins in vitro. *DNA Res* **7**, 143–150.

Petersen KR & Nerbonne JM (1999). Expression environment determines K^+ properties: Kv1 and Kv4 α-subunit-induced K^+ current in mammalian cell lines and cardiac myocytes. *Pflugers Arch* **437**, 381–392.

Qi SY, Riviere PJ, Trojnar J, Junien J-L & Akinsanya KO (2003). Cloning and characterization of dipeptidyl peptidase 10, a new member of an emerging subgroup of serine proteases. *Biochem J* **373**, 179–189.

Rhodes KJ, Carrell KI, Sung MA, Doliveira LC, Monaghan MM, Burke SL *et al.* (2004). KChIPs and Kv4 α subunits as integral components of A-type potassium channels in mammalian brain. *J Neurosci* **24**, 7903–7915.

Rocha CA, Nadal MS, Rudy B & Covarrubias M (2005). Inactivation coupled to deactivation: direct evidence of preferential closed-state inactivation in Kv4 channels. *Biophys J* **88**, 455A.

Ruschenschmidt C, Kohling R, Schwarz M, Straub H, Gorji A, Siep E *et al.* (2004). Characterization of a fast transient outward current in neocortical neurons from epilepsy patients. *J Neurosci Res* **75**, 807–816.

Schoppa NE & Westbrook GL (1999). Regulation of synaptic timing in the olfactory bulb by an A-type potassium current. *Nat Neurosci* **2**, 1106–1113.

Schrader LA, Anderson AE, Pfaffinger PJ & Sweatt JD (2002). PKA modulation of Kv4.2-encoded A-type potassium channels requires formation of a supramolecular complex. *J Neurosci* **22**, 10123–10133.

Serodio P & Rudy B (1998). Differential expression of Kv4 K^+ channel subunits mediating subthreshold transient K^+ (A-type) current in rat brain. *J Neurophysiol* **79**, 1081–1091.

Shibata R, Nakahira K, Shibasaki K, Wakazono Y, Imoto K & Ikenaka K (2000). A-type K^+ current mediated by the Kv4 channel regulates the generation of action potential in developing cerebellar granule cells. *J Neurosci* **20**, 4145–4155.

Spreafico F, Barski JJ, Farina C & Meyer M (2001). Mouse DREAM/calsenilin/KChIP3: gene structure, coding potential, and expression. *Mol Cell Neurosci* **17**, 1–16.

Strop P, Bankovich AJ, Hansen KC, Garcia KC & Brunger AT (2004). Structure of a human A-type potassium channel interacting protein DPPX, a member of the dipeptidyl aminopeptidase family. *J Mol Biol* **343**, 1055–1065.

Tkatch T, Baranauskas G & Surmeier DJ (2000). Kv4.2 mRNA abundance and A-type K^+ current amplitude are linearly related in basal ganglia and basal forebrain neurons. *J Neurosci* **20**, 579–788.

Van Hoorick D, Raes A, Keysers W, Mayeur E & Snyders DJ (2003). Differential modulation of Kv4 kinetics by KChIP1 splice variants. *Mol Cell Neurosci* **24**, 357–366.

Wada K, Yokotani N, Hunter C, Doi K, Wenthold RJ & Shimasaki S (1992). Differential expression of two distinct forms of mRNA encoding members of a dipeptidyl aminopeptidase family. *Proc Natl Acad Sci U S A* **89**, 197–201.

Watanabe S, Hoffman DA, Migliore M & Johnston D (2002). Dendritic K^+ channels contribute to spike-timing dependent long-term potentiation in hippocampal pyramidal neurons. *Proc Natl Acad Sci U S A* **99**, 8366–8371.

Xiong H, Kovacs I & Zhang Z (2004). Differential distribution of KChIPs mRNAs in adult mouse brain. *Mol Brain Res* **128**, 103–111.

Zagha E, Ozaita A, Chang SY, Nadal MS, Lin U, Saganich MJ *et al.* (2005). Dipepidyl peptidase 10 modulates Kv4-mediated A-type potassium channels. *J Biol Chem* **280**, 18853–18861.

Zaidi NF, Berezovska O, Choi EK, Miller JS, Chan H, Lilliehook C *et al.* (2002). Biochemical and immunocytochemical characterization of calsenilin in mouse brain. *Neuroscience* **114**, 247–263.

Zhou W, Qian Y, Kunjilwar K, Pfaffinger PJ & Choe S (2004). Structural insights into the functional interaction of KChIP1 with Shal-type K^+ channels. *Neuron* **41**, 573–586.

Acknowledgements

We thank Dr Lily Jan for providing us with the rat Kv4.2 cDNA, Dr William O. Cookson for the anti-DPP10 antibodies, and Aaron Lauver for technical assistance in preparing rat brain extracts. This work was supported by NRSA 133003317 (to H.H.J.), grant R01 NS31583, and grant P01 NS37444 from the National Institutes of Health.